学　位　論　文

EMT-driven cancer malignancy: what is the fundamental matter?

（EMT とがん悪性度：何が根本的事象なのか。）

2019 年 3 月

北　海　道　大　学

半田　悠

学　位　論　文

EMT-driven cancer malignancy: what is the fundamental matter?

（EMT とがん悪性度：何が根本的事象なのか。）

2019 年 3 月

北　海　道　大　学

半田　悠

Table of Contents

Table of Figures

List of Tables

1 Fundamental Publications for PhD thesis

- Haruka Handa, Ari Hashimoto, Shigeru Hashimot, and Hisataka Sabe.: **Arf6 and its ZEB1-EPB41L5 mesenchymal axis are required for both mesenchymal- and amoeboid-type invasion of cancer cells.**, *Small GTPases*, 420-426, 2018.

- Haruka Handa, Ari Hashimoto, Shigeru Hashimoto, Hirokazu Sugino, Tsukasa Oikawa, and Hisataka Sabe.: **Epithelial-specific histone modification of the miR-96/182 locus targeting AMAP1 mRNA predisposes p53 to suppress cell invasion in epithelial cells.** *Cell Communication and Signaling*, 16: 94, 2018.

2 Supportive Publications for PhD thesis

1. Menju T, Hashimoto S, Hashimoto A, Otsuka Y, Handa H, Ogawa E, Toda Y, Wada H, Date H, Sabe H.: **Engagement of overexpressed Her2 with GEP100 induces autonomous invasive activities and provides a biomarker for metastases of lung adenocarcinoma.** *PLoS One*, 6: e25301, 2011

2. Kinoshita R, Nam JM, Ito YM Hatanaka KC, Hashimoto A, Handa H, Otsuka Y, Hashimoto S, Onodera Y, Hosoda M, Onodera S, Shimizu S, Tanaka S, Shirato H, Tanino M, Sabe H.: **Co-overexpression of GEP100 and AMAP1 proteins correlates with rapid local recurrence after breast conservative therapy.** *PLoS One*, 8: e76791, 2013

3. Hashimoto S, Mikami S, Sugino H, Yoshikawa A, Hashimoto A, Onodera Y, Furukawa S, Handa H, Oikawa T, Okada Y, Oya M and Sabe H.: **Lysophosphatidic acid activates Arf6 to promote the mesenchymal malignancy of renal cancer.** *Nature Communications*, 7: 10656, 2016

4. Hashimoto A, Oikawa T, Hashimoto S, Sugino H, Yoshikawa A, Otsuka Y, Handa H, Onodera Y, Nam J M , Oneyama C, Okada M, Fukuda M and Sabe H.: **P53- and mevalonate pathway-driven malignancies require Arf6 for metastasis and drug resistance.** *Journal of Cell Biology*, 213: 81-95, 2016

5. Hashimoto A, Hashimoto S, Sugino H, Yoshikawa A, Onodera Y, Handa H, Oikawa T and Sabe H.: **ZEB1 induces EPB41L5 in the cancer mesenchymal program that drives ARF6-based invasion, metastasis, and drug resistance.** *Oncogenesis*, 5: e259, 2016

6. Otsuka Y, Oikawa T, Yoshino, Hashimoto S, Handa H, Yamamoto H, Hashimoto A, Sabe H.: **Frequent overexpression of AMAP1, an Arf6 effector in cell invasion, is characteristic of the MMTV-PyMT rather than the MMTV-Neu human breast cancer model.** *Cell Communication and Signaling*, 16: 1, 2018.

7. Oikawa T, Otsuka Y, Onodera Y, Horikawa M, Handa H, Hashimoto S, Suzuki Y, and Sabe H.: **Necessity of p53-binding to the CDH1 locus for its expression defines two epithelial cell types differing in their integrity.** *Scientific Reports*, 8: 1595, 2018

3 Conference Presentations

- Poster presentation. Haruka Handa, Shingo Takada, Yutaro Otsuka, Yasuhito Onodera, Tsukasa Oikawa, and Hisataka Sabe.: **Epithelial-mesenchymal transition accompanies mitochondrial fission and enhanced OXPHOS activity.**, Cold Spring Harbor Laboratory Meeting: Nutrient Signaling, 25th-28th October 2018, Cold spring harbor laboratory, New York, U.S.A.

- Oral presentation. Haruka Handa and Hisataka Sabe: EMT におけるミトコンドリア酸化的リン酸化制御とその役割，第１０回シグナルネットワーク研究会，29th-30th June, 2018, Kobe University, Kobe, JAPAN.

4 Abstract

Despite global intellectual efforts that have continued for over half a century, cancer is still an incurable disease. There are two main reasons for this difficulty; treatment resistance and metastatic recurrence. Recent studies revealed that these two phenomena are not mutually exclusive but intimately related with one another by an epithelial-mesenchymal transition, or EMT. During EMT, tumour cells that are originally from the epithelium alter their epithelial characters into mesenchymal traits, which are characterised by high motility and the ability for anchorage-independent survival. Almost two decades ago, clinical trials were conducted using protease inhibitors, and these were expected to be able to prevent tumour invasive activity. However, all of these trials ended up in poor results. This was as cancer cells are able to move without matrix proteases, which is referred to as an amoeboid-type cell invasion. Mesenchymal-invasion and amoeboid-invasion are interchangeable in response to surroundings, where cancer cells are exposed. In this thesis, the relation between the Arf6-AMAP1-EPB41L5 pathway (Arf6-pathway) and amoeboid-invasion was investigated. The Arf6 pathway was found by Professor Sabe's group, first in a malignant breast cancer, and has subsequently been shown to be involved in a variety of malignant tumours, including lung, head and neck, and renal cancer. This thesis further discovered that invasive breast cancer cells can exploit Arf6-pathway for their amoeboid motility.

The next question that this study looks at would be the differences that exist between mesenchymal cells experienced EMT and *bona fide* mesenchymal cells. Substantial evidence is emerging that EMT sometimes links to cell stemness. Normal p53 has a critical role in suppressing tumour progression in many ways. p53 negotiates EMT by transcribing miR-200 family to suppress transcription factors, such as ZEB1 and ZEB2,

which promote EMT. In this thesis, it has shown that p53 downregulates AMAP1, a core molecule of invasion machinery, via the miR-183 cluster. Thus far, it has been cleared that p53 cannot only target central proteins, such as transcription factors, but also implementation elements, including AMAP1. Those are mechanisms by which the epithelial cells employ p53, a reliable guardian, in order to prevent any aberrant motility. Professional mesenchymal cells, however, have high AMAP1 and low miR-183 cluster expressions, in spite of possessing a normal p53. This implies that *bona fide* mesenchymal cells may assign a different epigenetic status to cells that underwent EMT, at least in the sense of AMAP1 expression, even though both cells are phenotypically similar. These findings would thereby cast light on the complexity of the way in which cellular destiny would be decided.

While it is indubitably important to elucidate the mechanisms of gene expression reprogramming during EMT, there is a need to investigate EMT from another viewpoint as well. One unique principle of life is to extract energy from its environment, *viz*. metabolism. This thesis therefore attempts to explore the way in which cells harness metabolism in order to endure EMT. The main power plant in the cell is mitochondrion. Mitochondria build up their networks for efficient energy generation, and thus have dynamic morphology. It has already shown that EMT induces mitochondria fission with OXPHOS enhanced, and there is apparently a general agreement that mitochondria fission usually impairs OXPHOS activities, thereby leading to the paradox. This thesis advocates a plausible interpretation of this discrepancy.

5 Abbreviations

AMAP1: a multiple-domain Arf GAP protein 1

Arf: ADP-ribosylation factor

ATCC: American type culture collection

ATP: adenosine triphosphate

DMEM: Dulbecco's modified Eagle's medium

ECL: enhanced chemi-luminescence

EDTA: ethylenediaminetetraacetic acid

EFA6: exchange factor for Arf6

EGFR: epidermal growth factor

EMT: epithelial-mesenchymal transition

EMT-TF: EMT related transcription factor

EPB41L5: erythrocyte membrane protein band 4.1 like 5

GAP: GTPase activating protein

GEF: guanine nucleotide exchanging factor

GEO: gene expression omnibus

GEP100: guanine nucleotide-exchange protein 100 kDa

IRES: internal ribosome entry site

MMP: matrix metalloproteinase

MVP: mevalonate pathway

OCR: oxygen consumption ratio

OXPHOS: oxidative phosphorylation

PAGE: polyacrylamide gel electrophoresis

PBS: phosphate-buffered saline

PCR: polymerase chain reaction

PMSF: phenylmethanesulfonyl fluoride

PVDF: polyvinylidene difluoride

Rab: Ras related in brain

Ras: rat sarcoma

RT: reverse transcription

RTKs: receptor tyrosine kinases

SDS: sodium dodecyl sulfate

shRNA: short hairpin RNA

siRNA: short interference RNA

TBST: tris buffered saline with Tween-20

TCGA: the cancer genome atlas

TGF: transforming growth factor

UTR: untranslated region

WB: western blotting

WT: wild type

ZEB1: zinc finger E-box binding homeobox 1

6 Introduction

6.1 The importance of cancer research

Cancer has been the primary cause of death among the Japanese for the past three decades, followed by heart disease and pneumonia (Sakamoto et al 2018). It has also been responsible for approximately 9.6 million deaths globally and has become a major preoccupation in developed countries (Cancer Research UK). In 2000, cancer was the 9th largest cause of death globally, but in 2016, it was raised to the rank of 6th (Cancer Research UK). This is as developing countries solve their hygiene problems gradually through the support from advanced countries and the United Nations, the number of infectious diseases has decreased. Improved sanitation can prolong our lives, and is further attested to when the higher causes of death changes from infectious diseases to chronic diseases, such as cardiovascular disease and cancer.

In addition, tumours do not always occur with age. Each year, approximately 15,300 children are diagnosed with cancer. Although great progress has been made in adult cancer treatment, the number of childhood cancer cases has yet to decline in the last couple of decades. This situation must be ameliorated, as the human population can only be sustainable by fostering a healthy younger generation.

These days, cancer treatment places an economic burden on the world society. In Japan, the cost of cancer care alone occupies around 14% of annual medical expenditure, 4.2 trillion yen, and strains Japanese social welfare budget, which can subsequently wreak havoc on her economy (Sakamoto et al 2018). In order to prevent such a crisis, more intense research should be performed. Moreover, cancer research has a potential to not only ensure our society's sustainability but to also solve a piece of the most profound puzzle found in life.

One characteristic of cancer is its uncontrolled proliferation, which stems from cell-cycle dysregulation. From an evolutionary standpoint, in order to coordinate the entirety of their organs, multicellular organisms had to establish a more precise system that allowed a regulation of their proliferation rate. This was a markedly more complex process than what was needed with unicellular organisms. In other words, cancer cells retrieve their memory from the time when they led unicellular lives.

6.2 Tumour metastasis and EMT

Not only do tumour cells lose control on proliferation, but they also often lose their cellular identity: epithelial tumour cells often acquire motility to elicit metastasis (Nieto et al. 2016). As such, tumour metastasis is responsible for the high mortality ratio in cancer (Lambert et al. 2017). With no existing measure to control metastasis, a much deeper understanding of how and why cancer cells are able to transverse to distant organs is essential.

Metastasis occurs as a series of cellular action, which begins from invasion into basal lamina. At a point during tumour progression, cancer cells that are originally derived from epithelial cells convert themselves from epithelial-type to mesenchymal-type cells, thereby acquiring a migratory ability, which is referred to as epithelial-mesenchymal transition (EMT), as first described by Elizabeth Hay (Hay 1968). Indeed, EMT occurs not only in tumour progression but also in physiological processes, such as embryonic development and wound healing (Nieto et al. 2016).

EMT is provoked by pleiotropic signalling factors, including transforming growth factor beta (TGF-β), bone morphogenetic protein (BMP), epidermal growth factor (EGF), Wnt and Notch (Lamouille et al. 2014). Cellular changes during EMT are primarily

characterized by the loss of cell-cell adhesion, the loss of cell polarity, and the rearrangement of cytoskeletons in order to become capable of migrating away from the original epithelial sheets. There have been numerous studies on how cell junctions and polarity are deconstructed during EMT. One particular mechanism of disassembling adherence junction (AJ) involves the EMT-inducing signals causing the internalization of E-cadherin, the main component of AJ, which is mainly mediated by clathrin-dependent and clathrin-independent pathways (Lamouille et al. 2014). Epigenetic alterations are also found during EMT. Key transcription factors, ZEB1, SNAI1, SLUG (SNAI2) and TWIST1, which have been considered to be master regulators of EMT, thus bind to the promoter region of *CDH1* (the gene name of E-cadherin) and interact with the histone deacetylase (HDAC), inducing the repression of *CDH1* transcription (Lamouille et al. 2014). They also have a tendency to upregulate molecules, a characteristic of mesenchymal migratory cells, such as Vimentin and N-cadherin.

The biological sense of EMT could be regarded as the acquisition of motility. Actually, EMT-TFs promote expression of matrix-metalloproteinases (MMPs) with which tumour cells can negotiate a stromal meshwork dominated by type 1 collagen (Lamouille et al. 2014). This protease-dependent invasion is also referred to as mesenchymal-type invasion. In mesenchymal migration, cells elongate lamellipodia and filopodia to the leading edge and then integrins form cell-to-ECM interaction, namely focal adhesion (Friedl and Wolf 2003). For effective crawling, migrating cells use integrin recycling mechanisms, in which integrins binding with ECM are internalized by endocytosis and then recycled back to the leading edge (Muller et al. 2009). Moreover, it has been shown that these cells secrete MMPs at the frontal edge to generate a path in the stroma (Suzuki et al. 2011). In the 1990s, a variety of clinical trials that were aimed at MMPs were performed, but ended up in failure (Coussens et al. 2002). Intense research that reflected upon the dismal results

revealed that invasive cancer cells had another type of invasion, which is known as protease-independent invasion, or amoeboid-type invasion (Wolf et al. 2003). Indeed, the high contractility promoted by the ROCK signalling pathway enables cancer cells to squeeze themselves through the extracellular matrix (ECM) fibres (Friedl and Wolf 2003). Interestingly, mesenchymal- and amoeboid-type invasion are mutually interchangeable, but not exclusive. Therefore, inhibiting both types of invasion would be needed but this requires an in-depth understanding.

As illustrated in this study, the multifaceted regulation in EMT and its roles exist; a complexity that still intrigues many scientists.

6.3 Arf6-AMAP1 pathway on Tumour Malignancy

A number of mechanisms on cancer malignancy have been identified so far. One of the more well-known mechanisms is the growth factor signalling that involves receptor tyrosine kinases (RTKs) or G protein-coupled receptors (GPCRs). Aberrant enhancement of these pathways constitutes a major cause for augmented proliferation, survival and motility.

Our team, led by Professor Sabe, has identified a molecular link between the RTK activation and invasiveness, namely, the Arf6-AMAP1-EPB41L5 pathway (Sabe et al. 2009).

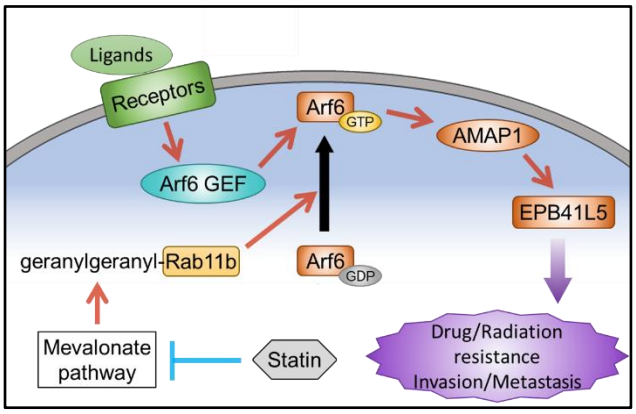

Figure 6-1. The scheme of Arf6-AMAP1-EPB41L5 pathway

Arf6 is a class-III protein in the Arf superfamily and is involved in membrane trafficking and remodelling (Donaldson and Jackson 2011). The activation of RTKs, including EGFR and HGFR, recruits GEP100, a GTP-exchanging factor (GEF) for Arf6, for their phosphorylated tyrosine residues (Morishige et al. 2008). The activated Arf6 then employs AMAP1 to bind EPB41L5, which promotes EMT and integrin recycling (Hirano et al. 2008, Onodera et al. 2012, Onodera et al. 2013). We have already shown that the lysophosphatidic acid (LPA) receptor, a GPCR, can also recruit EFA6 and promote tumour cell invasiveness via Arf6-AMAP1-EPB41L5 pathway (Hashimoto et al. 2016). To be activated by RTKs or GPCRs, Arf6-GDP should be trafficked to the plasma membrane, which is mediated by the geranylgeranylated Rab11b (Hashimoto et al. 2016b). We have shown that statins can reduce this geranylgeranylation by inhibiting HMG-CoA reductase, which is the main enzyme of the mevalonate pathway (Hashimoto et al. 2016b). Therefore, *in vivo* experiments with statin could bring forth positive and meaningful results pertaining to the reduction of tumour burdens that are driven mainly by this pathway.

Our group has recently reported that this pathway is responsible for treatment-resistance, i.e., chemo- and radio-resistance (Hashimoto et al. 2016b, Onodera et al. 2018). Mechanistically, malignant breast cancer cells exploit this pathway in order to promote anterograde transportation of mitochondria, leading to the avoidance of oxidative catastrophe by radiation (Onodera et al. 2018).

Our team is thus currently trying to understand how to treat cancer that is highly addicted to this pathway. Considering the central roles of mitochondria in cellular functions and the involvement of this pathway in mitochondria dynamics, we envision that targeting this pathway has the potential to circumvent the resistance.

6.4 The cooperation of p53 and microRNA against EMT

In human cancer, the most frequently mutated gene is *TP53.* In a normal physiological condition, p53, the protein product of *TP53*, is activated by various stress signals and executes anti-proliferative programmes, such as cell cycle arrest, cellular senescence and apoptosis (Kastenhuber and Lowe 2017). Therefore, p53 has been titled as the genome guardian. Additionally, p53 plays a regulatory role in cellular metabolism and antioxidative statuses (Kruiswijk et al. 2015). Recent studies have also revealed a novel function of p53, which would be in restricting epithelial cell plasticity. For example, during physiological EMT, p53 can coordinate neural crest delamination (Rinon et al. 2011). Consistently, the dysfunction of p53, as seen in tumour cells, can lose the stability of epithelium and could cause dedifferentiation to cancer stem-like cells (Mizuno et al. 2010). It has been demonstrated previously that mesenchymal features by EMT are sometimes associated with stem cell properties (Mani et al. 2008). In this event, loss of p53 is responsible for the downregulation of microRNAs (miRNAs) that target EMT-transcription factors (EMT-TFs), including ZEB1, SNAI1, SNAI2 and BMI1 and stemness-related factors (Chang et al. 2011, Kim et al. 2011b, Nieto et al. 2016). As described, p53 is broadly involved in cellular function. We have already documented the link between p53 mutations and Arf6-AMAP1-EPB41L5 pathway (Hashimoto et al. 2016b). In some breast cancer cells, the loss of normal-p53 can induce ZEB1, which can sequentially induce EPB41L5 (Hashimoto et al. 2016a).

The miRNA gene is first transcribed into a primary miRNA (pri-mRNA), which is then processed by the microprocessor complex comprising of RNase III enzyme called Drosha and subsequently cleaved by Dicer into functional mature miRNA (Gebert and MacRae 2018). Messenger RNAs (mRNAs) have miRNA binding sites in their 3’ untranslated

region (UTR) with strong complementarity to miRNA. These bindings can result in translational repression and degradation of the target mRNA molecule, and thus, miRNA is generally involved in gene silencing. Although the miRNA to mRNA complementarity is strong, a miRNA does not have any one-to-one correspondence to a specific mRNA; one mRNA can be targeted by many miRNAs. This one to multi relation enables miRNAs to fine-tune protein expression. Complex organisms are thought to utilize miRNAs to moderately regulate a wide range of biological processes, including differentiation, cell metabolism and apoptosis (Gebert and MacRae 2018). Dysregulation of an individual or a subset of miRNAs would lead to a variety of human diseases, such as cancer, cardiovascular diseases, and metabolic disorders (Li and Kowdley 2012). Recently, miRNAs have been classified into oncomiR or anti-oncomiR in tumour biology, depending on each expression level, but these two classes are not necessarily an alternative for any subsets of miRNA; while the miR-183 works as a tumour suppressor in lung cancer, this miRNA is involved in tumour progression in prostate cancer (Dambal et al. 2015, Peng and Croce 2016). This implies that a group of miRNAs is not limited to each specific cellular function, such as motility, proliferation, and metabolism.

6.5 Mitochondria Dynamics and OXPHOS

It would not be exaggerated to state that eukaryotic cell activities largely rely on mitochondria, which has a double lipid membrane and whose inner membrane are folded inwards (cristae). They govern metabolic systems for cellular survival and proliferation, as well as function as a death signal for the appropriate demise of deviating cells (Westermann 2010). One of the main systems in mitochondria is the tricarboxylic acid (TCA) cycle, into which the oxidative metabolism of carbohydrates, amino acids, and

fatty acids converge. TCA cycles produce reduced coenzymes, nicotinamide adenine dinucleotide (NADH) and flavin adenine dinucleotide ($FADH_2$), which are then re-oxidized through electron transport chain (ETC).

Mitochondria are not static but highly dynamic organelles, being different from what was depicted as small, static ovoid organelles (Wai and Langer 2016). The balance of fusion and fission are typically countered with each other; when fusion is inhibited, fission progresses, and vice versa. Mitochondrial fusion is performed through a two-step process. Firstly, the outer mitochondrial membrane is catalysed by mitofusins 1 and 2 (MFN1 and MFN2), which forms homo-oligomeric and hetero-oligomeric complexes. Next, optic atrophy gene 1 (OPA1) promotes inner mitochondrial membrane (IMM) fusion (Chan 2012) (Fig. 6-2).

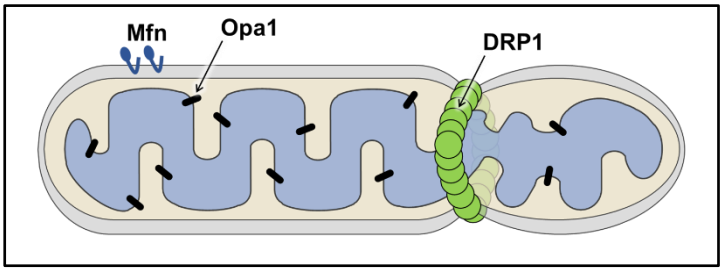

Figure 6-2. The scheme of mitochondria fission
Mitochondria fission is mediated by DRP1.

Mitochondrial fission is a multi-step process in which dynamin-related protein (DRP1), whose role is analogous to dynamin in endocytic vesicle fission, appears to be a central player (Chan 2012). During mitochondria fission, a tubule from the endoplasmic reticulum (ER) is recruited to the mitochondria fission site. This site would be previously marked by mitochondrial DNA (mtDNA). The tubule then wraps around the site for mitochondrial constriction (Tilokani et al. 2018). This mitochondria-ER contact site allows the DRP1 to gather and build complexes which would lead to mitochondrial fission

(Tilokani et al. 2018). However, it has been demonstrated that DRP1 cannot terminate mitochondrial fission, so the final step would still need to be investigated.

For cells to maintain their lives, mitochondria dynamics and energy production are both essential. The main source of cellular energy is adenosyl triphosphate (ATP), which is generated by glycolysis and the TCA cycle. The amount of ATP production by TCA cycle is around 20 times higher than that of glycolysis, although this would require oxygen. Indeed, NADH and $FADH_2$ from the TCA cycle require re-oxidization for another oxidation of metabolites. These two coenzymes donate their electrons to a set of electron carriers called ETC, where a pair of electrons loses a large amount of free energy and combines with the oxygen and proton into water. The ETC is composed of Complexes I, II, III, IV, and V (Fig. 6-3). Complex I, NADH dehydrogenase, oxidizes NADH and transfers its electron to coenzyme Q (CoQ). Complex II is succinate dehydrogenase, a member of TCA cycle, which catalyses succinate to fumarate, as FAD is reduced to $FADH_2$. CoQ is also a transferred electron from $FADH_2$. The electrons are passed on to complex III and IV, both of which are cytochromes and contain a heme group (a porphyrin ring plus iron). The final step of the ETC would be the generation of water from electrons, oxygen, and hydrogen. An incomplete reduction of oxygen can sometimes occur and leads to the production of reactive oxygen species, such as superoxide and hydroxyl radicals, which can damage DNA, protein, and lipid. These electron transfers are coupled with proton transport from the mitochondria matrix to the intermembrane space, making an electrical gradient. This proton gradient has the potential to drive complex V, ATP synthase or F_1/F_0 ATPase generating ATPs. Therefore, a series of ETC and ATP production are called oxidative phosphorylation (OXPHOS). Furthermore, it has been reported that non-functional mitochondria lose their electrical gradient and are degraded

by mitophagy (Youle and Narendra 2010).

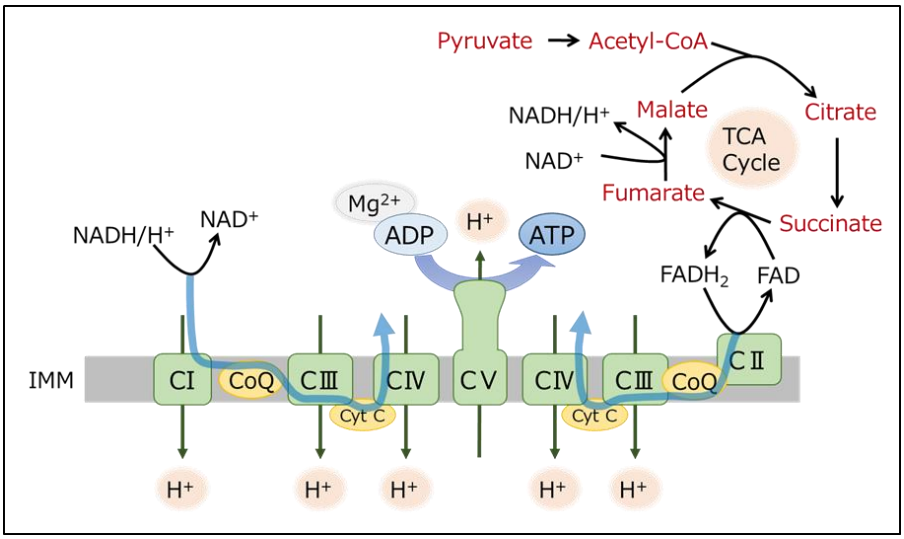

Figure 6-3. The electron transport chain

Blue arrow stands for the flow of the electron.

It has been long believed that tumour cells have impaired mitochondria and are thus heavily dependent on glycolysis, even in the presence of sufficient oxygen (Warburg effect or aerobic glycolysis), a theory that was first hypothesized by Otto Warburg almost a century ago (O. Warburg 1931). However, it has now been realised that mitochondria in cancer cells are indeed functional (Vander Heiden et al. 2009). Using TCA cycle and its downstream ETC means that ROS generation will be inevitable. Therefore, cancer cells have to prevent negative effects from this ROS. Our group has demonstrated that malignant breast cancer cells utilise the Arf6-AMAP1 pathway to promote the anterograde trafficking of mitochondria (Onodera et al. 2018). The blockade of this pathway thus causes aggregation of mitochondria and could trigger detrimental effects through a ROS-induced ROS release-like mechanism.

6.6 Tools used for measuring Oxygen Consumption Ratio

In mitochondria, oxygen is mainly consumed by the electron transfer system consisting of four complexes (complex I, II, III, and IV), which contributes to the electrochemical proton gradient and eventually to the production of ATP (Fig).

Figure 6-4. Oxygraph-2k

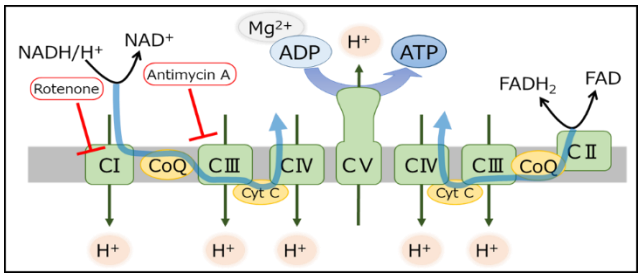

Figure 6-5. The electron transfer chain

Rotenone and Antimycin A inhibit Complex I and III, respectively.

As such, this chain of flow is dubbed as oxidative phosphorylation (OXOHOS). The main purpose of measuring oxygen consumption ratio (OCR) would be to assess the activity of oxidative phosphorylation. There are two systems that can measure OCR changes in the respiration rate of mitochondria; one is high-resolution Oxygraph-2k (O2k: Oroboros) and the other is the sensitive high-throughput Seahorse XF Extracellular Flux Analyzer. In the experiments enacted for this thesis, Oxygraph-2k was used. Thus, I will describe the features of this system below.

O2k measures oxygen concentration by polarographic sensors is based on a chemical redox reaction. Operators must directly inject the substrates to isolated mitochondria or cells that are suspended in the solution. For example, malate, pyruvate, and glutamate are for complex I and a further injection of succinate is performed for the assessment of the electron transfer through complex I and II.

6.7 The Aims of This Thesis

EMT is an important process for normal epithelial cells during embryogenesis and the healing of wounds. Although some studies have revealed that EMT is not indispensable for cancer cell metastasis (Fischer et al. 2015, Zheng et al. 2015), it has also been found that cancer cells utilise EMT for anoikis, chemo-resistance, and stemness (Nieto et al. 2016). Therefore, the three studies listed below were conducted with the aim of elucidating the potential link between these traits and the relevance of the Arf6-AMAP1 pathway.

The first study examines whether the Arf6-AMAP1 pathway is involved in the amoeboid-type cell invasion. The second study tries to understand the different role of p53-miRNA axis on cell invasion, especially in epithelial cells and fibroblasts. The third study seeks to provide a novel insight into the relation between EMT and mitochondria bioenergetics in normal cells.

It is to be noted that the first and third studies are intimately connected as the EMT is the key event to cancer malignancy and would thus require investigation from various viewpoint. However, the second study does not share a strong relation with the others but connects via EMT as the study is focused on the difference between the epithelial cells undergoing EMT and the *bona fide* mesenchymal cells.

1. Investigate the role of Arf6-AMAP1 pathway in amoeboid-type invasion
    a) Induction of amoeboid morphology by a protease inhibitor cocktail
    b) Amoeboid-invasion assay by stimulating RTK and GPCR signalling

2. Investigate the mechanism on p53 function against AMAP1-based tumour invasion

   a) Searching for miRNAs by using microarray among MDA-MB-231 cells with different p53 statuses

   b) TCGA analysis mining for miRNAs that correlates with AMAP1

   c) Confirmation of miRNAs' expression between transformed cells and non-transformed cells

   d) Assessment of miRNA and AMAP1 expression among epithelial-type cells, mesenchymal-type cells and original mesenchymal cells

3. Investigate the relation of EMT and mitochondria on non-transformed cell

   a) Assessment of the oxygen consumption ratio during EMT

   b) Search for the key molecule that causes OXPHOS enhancement during EMT

   c) Formulation of the model between OXPHOS and mitochondria dynamics during EMT

7 Materials and Methods

7.1 Cell Culture

The cell lines used in this thesis are listed in Table 7-1, along with their culture media and histology. Cells were passaged and fed with fresh media before they were confluent. All the assays with cell lines in this thesis were conducted within a range of 15 passages from thaw. Only the MDA-MB-231 cells were incubated in 7.5% CO_2 at 37 °C, while the other cells were in 5% CO_2 at 37 °C. The number of cells was counted by using Countess® II FL (Thermo Fisher Scientific).

Table 7-1. Cell lines

Cell line	Culture media	Histology	Source
293FT	DMEM (SIGMA) with 10% FCS (Corning)	-	ATCC
HEK293T	DMEM (SIGMA) with 10% FCS (Corning)	-	ATCC
MDA-MB-231	DMEM, RPMI with 10 % FCS and 5 % Nu supplemented 2 mM Glutamine	a pleural effusion of a breast adenocarcinoma	ATCC
MCF7	DMEM (SIGMA) with 10% FCS (Corning)	a pleural effusion of a breast adenocarcinoma	ATCC
Panc1	DMEM (SIGMA) with 10% FCS (Corning)	pancreatic epithelioid carcinoma	ATCC
MiaPaca2	DMEM (SIGMA) with 10% FCS (Corning)	pancreatic cancer	ATCC
A549	DMEM (SIGMA) with 10% FCS (Corning)	lung adenocarcinoma	ATCC
NMuMG	DMEM (SIGMA) with 10% FCS (Corning) supplemented with 10μg/ml of Insulin	normal murine mammary grand	ATCC

The p53 derivatives of MDA-MB-231 cells were generated previously, and the NMuMG cells and A549 cells with overexpressed mitoNEET or mitoNEET-HA were produced by expression vectors. Refer to section 7.4 for more details.

Cell viabilities were assessed by using Cell count kit-8 (Dojindo). 1.0×10^4 of cells were plated onto 96 well plates. After 24 hours of incubation, the cells were cultured with a cell count reagent for 2 hours and then the absorbance of 595 nm of the medium was measured by the luminometer (ARVO MX 1420 Multilabel Counter; PerkinElmer).

7.2 **Amoeboid invasion assay and quantification**

All assays for amoeboid invasion and morphology quantification were performed by using 1 mg/ml fibrillar type-I collagen gels, which were prepared from a 3mg/ml collagen solution, 4 × DMEM, 0.1 N NaOH, and double-distilled water. For the morphology assay, MDA-MB-231 cells were cultured on the culture dish, which was pre-coated by fibrillar collagen gels either with or without a Pi mix. After 2 days of incubation, the cells were observed using a microscope (EVOS FL Cell Imaging System). 1.0×10^5 of MDA-MB-231 cells which were pre-treated with the indicated siRNAs were seeded with a PI mix onto the top of fibrillar collagen gels, which were then set within the upper chamber of a 24-well Transwell plate (8 μm pore size; Corning). The lower chamber was filled with a medium that contained 2 ng/ml of LPA or 10 ng/ml of EGF. After 3 days of incubation, cells were stained with 4 μM calcein-AM (Dojindo), and z-section images from the top of collagen gels down to 100 μm deep at every 5 μm intervals were acquired using a confocal microscope (Nikon A1R), equipped with a Plan Fluor 10 objective, and were analysed by the NIS-Elements (Nikon Software). Invasion activities were quantified as

the percentage of cells existing between 40 μm to 100 μm of the collagen gels, in which 2 different fields were counted within 2 independent experiments.

7.3 siRNA

All siRNAs are listed on table 3-5. For the transient siRNA-mediated gene silencing, 2.0 × 10^5 of cells were seeded on the 6cm diameter of culture dish (Corning) and transfected at the same time as the final 50 nM siRNAs by using RNAiMAX (Thermo Fisher Scientific), according to manufacturer's instruction. Each siRNA transfection was done 48 hours prior to the assays. For each experiment, Stealth RNAi duplex with medium GC content (Invitrogen) or ON-TARGET plus Non-targeting Pool (D-001810-10; Dharmacon) was used as a negative control.

The siRNAs for GEP100, AMAP1, Arf6, EPB41L5 were synthesized by Japan Bio Services Co., LTD., while the other siRNAs were purchased from Dharmacon.

Table 7-2. Sequences of siRNA The sequences of Stealth RNA1 and SMART pool were confidential unless users purchased them.

siRNA target	Sequence (5' to 3') or ID
GEP100	GUGAAAUCACUGGCCGAGU
AMAP1	GACCUGACAAAAGCCAUUA
ARF6	GCACCGCAUUAUCAAUGACCGUU
EPB41L5 #1	GAGAUGGAACUGGCUAUUUUU
EPB41L5 #2	UUCAGAUUCGUGCCUAUUCAG
ZEB1 #1	Stealth RNAi (HSS110548)
ZEB1 #2	Stealth RNAi (HSS110549)
mitoNEET (mouse)	ON-TARGET plus siRNA – SMART pool (Dharmacon) L-063953-01
mitoNEET (human)	ON-TARGET plus siRNA – SMART pool (Dharmacon) L-020954-01

7.4 Plasmid constructs and transfection

p53 manipulation

For the stable silencing of the endogenous mutant p53, shRNAs against p53 (TRCN0000342261) was purchased from the manufacturer (Sigma Mission; Sigma-Aldrich). pLKO.1-puro–based recombinant lentiviruses were generated by transfecting the pLKO vectors, the envelope plasmid pMD2.G (12259; Addgene) and the packaging plasmid psPAX2 (12260; Addgene) into 293FT cells. Lipofectamine LTX (Invitrogen) was used for pLKO-series plasmid transfection. 48 hours after transfection, the supernatant medium was harvested and filtered through 0.45-μm filters (Advantec). The lentivirus preparations were infected to target cells in the presence of 8 μg/ml Polybrene. To select the infected cells, 1.25 μg/ml of puromycin was added to the culture medium 24 hours after the infection (Hashimoto et al. 2016b).

In order to generate the cells stably expressing recombinant p53 (shp53/wt), pBabe-hygro vector based retroviruses were used. Plasmid that encoded the V5-tagged normal p53 protein was purchased (22945; Addgene). DNA fragments of this normal p53 was ligated into the SnaB1 site of pBabe-hygro vector. Retroviruses were also produced using Plat-E packaging cells and the pGP-Ampho and pE-Ampho plasmids (Takara Bio Inc.) (Akagi et al. 2003).

Twenty-four hours after the infection, the cells were by the addition of 200 μg/ml hygromycin (Wako Pure Chemical Industries) and 1.25 μg/ml puromycin.

mitoNEET manipulation

The backbone of pPB, a piggyBac transposon vector system, was exploited to generate mitoNEET expressing cells. For the stable expression vectors, a hybrid of the EF1α and HTLV promoters with the upstream CMV enhancer (CEH), multiple cloning sites (MCS),

and the HSV TK polyA sequence were systematically inserted into the pPB-vectors (Onodera et al. 2018). Between the MCS and polyA sequences, the gene encoding puromycin N-acetyltransferase (pac) was inserted, following an internal ribosome entry site (IRES) of EMCV. The cDNAs encoding human mitoNEET/CISD1 or mouse mitoNEET/Cisd1 with restriction enzyme site of BamH1 and Not1 at both ends were amplified by the Taq polymerase (Roche) from the first strand of A549 cells and NMuMG cells, respectively. These were also ligated into the pcDNA5/FRT vector (Invitrogen). Their sequences were checked and sub-cloned into BamH1 and Not1 site of pPB-CEH-MCS-IP. For the construction of HA-tagged mitoNEET, genes encoding mitoNEET were amplified without their stop codon and ligated with HA gene. Each pPB-vector was co-transfected with the hyperactive piggyBac transposase (Yusa et al. 2011) into target cells through the use of ViaFect (Promega), in accordance with manufacturer's instruction. After 48 hours, the cells were selected by puromycin (1 μg/ml).

All the PCR steps were performed with Verti 96 well Thermal Cycler (Applied Biosystems; AB)

7.5 **Microarray analysis**

MDA-MB-231 cells with parental p53, shp53 or shp53/wt were serum-starved for 16 hours and were then either untreated or treated with 2 ng/mL of TGF-beta1 for 2 hours. Total cellular RNAs was purified using the QIAGEN RNeasy Mini Kit (QIAGEN,), following the manufacturer's instructions. Microarray analysis of miRNA expression from total cellular RNAs was performed by Toray. Java TreeView software was used for the colour visualization of the data.

7.6 Dual luciferase reporter assay

In the dual luciferase reporter assay system (Promega), the activities of firefly (*Photinus pyralis*) for targets and Renilla (*Renilla reniformis*) luciferases for internal controls were measured sequentially from a single sample, and contributed to an exclusion of distributed transfection. All activities of firefly were normalised to Renilla as the internal control.

By using Lipofetamine LTX (Invitrogen), HEK293T cells were transiently transfected with pEZX-MT01 target reporter plasmids that contained the full length of wild-type AMAP1 3'-UTR and its mutants without the miRNA target sequences, all of which were purchased from GeneCopeia. These cells were simultaneously transfected with the oligonucleotide precursors of hsa-miR-96, hsa-miR-182, or hsa-miR-301a (Ambion). 5.0×10^4 cells were then cultured into a 24-well plate. 24 hours after the transfection, luciferase assays were performed through use of the luminometer (ARVO MX 1420 Multilabel Counter; PerkinElmer).

7.7 RNA extraction and complementary DNA synthesis

RNA was extracted by using TRIsol Reagent (Invitrogen) or RNeasy Kit (QIAGEN). In the case of TRIsol, RNA extract was first mixed with chloroform and incubated on ice for 15 minutes. Post incubation, the lysate was centrifuged at 12,000 rpm for 15 minutes at 4℃, in order to separate the mixture into the upper aqueous and the lower phenol layer. The upper phase that contained RNA was next mixed with isopropanol and centrifuged at 12,000 rpm for 15 minutes at 4℃, to be precipitated. RNeasy kit was used in accordance with the manufacturer's instruction and the RNA concentration was measured with NanoDrop Lite (Thermo Fisher Scientific).

Furthermore, complementary DNAs (cDNAs) for cloning were synthesized by SuperScript IV. Firstly, 1 μg of RNA, 10 mM deoxynucleotides (dNTPs), and 50 μM random hexamers were mixed together and heated at 65℃ for 5 minutes, and then incubated on ice for 3 minutes. Next, the RNA mixture was combined with SSIV buffer, 100 mM DTT, ribonuclease inhibitor and SSIV reverse transcriptase. Finally, the whole mixture was incubated at 23℃ for 10 minutes, and heated at 55℃ for 10 minutes, and incubated at 80℃ for 10 minutes in order to halt the reaction. For the qPCR of mRNA and miRNA, the cDNA was produced by the SuperScript VILO (Invitrogen) and TaqMan Reverse Transcription Reagents (Applied Biosystems), as per the manufacturer's instruction.

7.8 Quantitative real time-polymerase chain reaction (qRT-PCR)

qPCR for the final 5 ng of RNA was performed through use of the TaqMan system (Applied Biosystem). The TaqMan probes for qPCR assay was listed in table 7-3, and the machine programme is set as per table 7-4.

Table 7-3. Assay IDs of TaqMan probes

Target DNA	Assay ID
Actin b	Mm02619580_g1
mitoNEET/Cisd1	Mm01172641_g1
AMAP1/ASAP1	Hs00535362_s1
GAPDH	Hs02758991
hsa-miR-182	002334
hsa-miR-96	000434
USB1	Hs00984809_m1

Table 7-4. The qPCR programme *means the timing of data collection.

microRNA			messengerRNA		
95℃	10 min	× 1	50℃	2 min	× 1
95℃	15 sec	× 40	95℃	20 sec	× 1
60℃ *	1 min		95℃	3 sec	× 40
			60℃ *	30 sec	

7.9 Western blotting and ECL

For SDS-PAGE, all cells were grown to nearly 90% confluency. Cells were washed with ice-cold PBS twice, then lysed with an appropriate volume of GGA buffer or RIPA buffer (table 7-5) that was supplied with protease inhibitors (table 7-6) and incubated on ice for 10 minutes. After incubation, cell lysates were centrifuged at 15,000 *g* for 30 minutes at 4℃. Supernatants from centrifuged samples were transferred to a new 1.5 ml sized microcentrifuge tube, and protein concentration was detected by using the Bradford Assay (BioRad). Samples were stored at -80℃.

Table 7-5. The components of GGA buffer and RIPA buffer

GGA buffer		**RIPA buffer**	
Component	Final conc.	Component	Final conc.
Tris-Cl (pH 8.0)	50 mM	Tris-Cl (pH7.5)	10 mM
NaCl	100 mM	EDTA	5 mM
$MgCl_2$	10 mM	NaCl	150 mM
Triton X-100	1.0%	Triton X-100	1.0%
Sodium cholate	0.050%	Sodium deoxycholate	1.0%
Sodium Dodecyl Sulfate	0.0050%	Sodium Dodecyl Sulfate	0.1%
Glycerol	10%	Glycerol	10%
dissolved into double distilled water		dissolved into double distilled water	

Table 7-6. The cocktail of protease inhibitors

Protease Inhibitors	
Component	Final conc.
Aprotinin	0.01%
Leupeptin	0.01 μM
Pepstatin A	0.01 μM
PMSF	0.01 mM
Na_3VO_4	0.02 mM
DTT	2 mM

The SDS-gels are composed of two different gels. The upper gel is used for the stacking of protein samples, and the lower gel is for separating samples by their molecular weight. The SDS-polyacrylamide gels were self-made and the concentration of gels was decided by the molecular weight of the protein. In this case, I used 15% gel for proteins under 20 kDa, 10% gel for 20 to 50 kDa and 8% gel for over 50 kDa. The separating gel components of each concentration are listed in table 7-7 and table 7-8 is for the stacking gel (Kielkopf et.al., 2012).

Table 7-7. The components of separating gel

Percentage of Separating gel	8%	10%	15%
H_2O	4.6 mL	4.0 mL	2.3 mL
30% acrylamide	2.7 mL	3.3 mL	5.0 mL
1.5 M Tris (pH 8.8)	2.5 mL	2.5 mL	2.5 mL
10% SDS	0.1 mL	0.1 mL	0.1 mL
10% ammonium persulfate	0.1 mL	0.1 mL	0.1 mL
TEMED	0.006 mL	0.004 mL	0.004 mL
Final Volume	10 mL		

Table 7-8. The components of stacking gel

Stacking gel	mL
H_2O	2.1
30% acrylamide	0.5
1.5 M Tris (pH 8.8)	0.38
10% SDS	0.03
10% ammonium persulfate	0.03
TEMED	0.003
Final Volume	10

Table 7-9. The recipe of sample buffer

SDS-sample buffer	Final conc.
Glycerol	50%
Tris-Cl (pH 6.8)	250 mM
DTT	500 mM
SDS	10%
Bromophenol blue	0.05%
H_2O	-

All the samples for western-blotting were prepared with a SDS-sample buffer (Table 7-9) and applied to the gel with a concentration that is proper for the proteins of interest. SDS-PAGE was run at a constant current (25 mA / gel) for almost 90 minutes and western-blotting (WB) was run at a constant voltage of 150 V for two hours. For the blotting of proteins, polyvinylidene difluoride (PVDF) membrane (Immobilon-P; Millipore), with a pore size of 0.45 μm, was used.

After the western-blotting, each membrane was blocked for 1 hour with blocking buffer, which could be 5% skim milk or 5% bovine serum albumin (BSA) in tris-buffered saline and polysorbate 20 (TBS-T), depending on 1st antibody (also see Section7.11). Then, these membranes were incubated with each antibody for the protein of interest in 2% of blocking buffer overnight. After the incubation, these membranes were washed with TBS-T three times and reacted for an hour with a secondary antibody conjugated with horse radish peroxidase (HRP). Finally, the ECL solution (GE healthcare) was applied to membranes, and their enhanced chemiluminescent was detected by X-ray film (Fuji). To quantify the levels of ECL, Image J software was used.

7.10 **Mitochondrial respiration**

The oxygen consumption ratio was measured through using Oxygra-2k, as stated in chapter 5. Cells were harvested with trypsin and spun down at 700 rpm for 2 minutes at 25℃. Then cells were then washed with PBS, spun down at 700 rpm for 2 minutes at 25℃ and suspended with MiR05 buffer (table 7-11). 500 μL of cell suspension was applied to one chamber of O2k. The number of cells was counted by Countess® II FL. The reagents were then added by a Hamilton syringe in order of table 7-10 and the chronological change of OCR was monitored. The average values of OCR in stability were used for subsequent analyses. The OCR in Glutamate addition was used as the complex-I dependent OXPHOS, and the OCR in succinate was used as complex-I and II related OXPHOS.

Table 7-10. Reagents for OCR measurement

1	Malate + Pyruvate
2	ADP + Mg
3	Glutamate
4	Cytochrome C
5	Succinate
6	FCCP
7	Rotenone
8	Antimycin A

Table 7-11. The recipe of MiR05 buffer

Components	Concentration in use
EGTA	0.5 mM
Taurine	20 mM
$MgCl_2$	3 mM
Sucrose	110 mM
K-lactobionate	60 mM
KH_2PO_4	10 mM
K-HEPES	20 mM
BSA	1 mg/mL
pH	7.1

7.11 **Antibodies**

The antibodies used in this thesis are listed in table 7-12.

Table 7-12. The list of antibodies used in this thesis

Target	Host	Dilution for WB	Blocking Solution	Obtained from
ARF6	mouse	1/1000	BSA	Original
GEP100	rabbit	1/1000	skim	Original
AMAP1	rabbit	1/2000	skim	Original
EPB41L5	rabbit	1/4000	skim	Original
p53	mouse	1/1000	skim	Cell Signalling Technology
E-cadherin	mouse	1/1000	BSA	BD Transduction Laboratories
Vimentin	rabbit	1/1000	BSA	Cell Signalling Technology
phosphor-Smad2	rabbit	1/1000	BSA	Cell Signalling Technology
beta-actin	mouse	1/5000	skim	SIGMA
mitoNEET (human/mouse)	rabbit	1/1000	skim	Original

7.12 **Reagents**

Reagents in this thesis are listed below (table7-13).

Table 7-13. Reagents used in this thesis

Reagent	Obtained from	Condition in Use
bovine collagen solution, type-I, 3 mg/mL	Advanced BioMatrix	See 7.2
GM6001	Santa Cruz Biotechnology	50 mM in PI mix
E64	Sigma-Aldrich	250 mM in PI mix
pepstatin A	Sigma-Aldrich	100 mM in PI mix
aprotinin	Sigma-Aldrich	2.2 mM in PI mix
leupeptin	Sigma-Aldrich	2 mM in PI mix

lysophosphatidic acid	Santa Cruz Biotechnology	5 nM
epithelial growth factor	PeproTech	10 ng/mL
transforming growth factor	PeproTech	5 ng/mL
insulin, human recombinant	Wako	100 ng/mL

PI mix indicates protease inhibitor mixture (see Chapter 8).

7.13 **Statistical analysis**

All statistical analyses were conducted with an unpaired *t*-test by using the Prism 6 (GraphPad), unless another method is stated. A P-value of under 0.05 was regarded as statistically significant.

8 Arf6-AMAP1 pathway under EMT is required for amoeboid-type invasion of cancer cells

8.1 Introduction

The small GTPase Arf6 is necessary for cell motility. Arf6 and its downstream proteins are often overexpressed in some kinds of tumours, including the breast, kidney, head and neck, and lung, and is attributed to their malignancy, such as the mesenchymal invasion and radiotherapy resistance (S. Hashimoto et al. 2016, Kinoshita et al. 2013, Menju et al. 2011, Onodera et al. 2018, Otsuka et al. 2016, Sato et al. 2014).

Cancer cell invasion is mainly classified into two types: mesenchymal-type invasion and amoeboid-type invasion (Wolf et al. 2003). It has already been reported that these types of invasion are able to convert into one another, which is referred to as a mesenchymal-amoeboid transition (MAT). I have thus examined the role of Arf6-AMAP1 pathway on amoeboid invasion.

8.2 Results

Malignant breast cancer cells can alter their morphologies under protease inhibitors

MDA-MA-231 cells were seeded on fibrillar collagen in the presence of a protease inhibitor cocktail (PI mix). Without the PI mix, the morphology of most cells was in an elongated-form, which was characterized as an invasive mode. On the other hand, when cultured under PI mix, they altered their shape into a rounded form (Fig. 8-1). These results are consistent with previous reports (Wolf et al. 2003), that had suggested that malignant cells can change their shape depending on their environment.

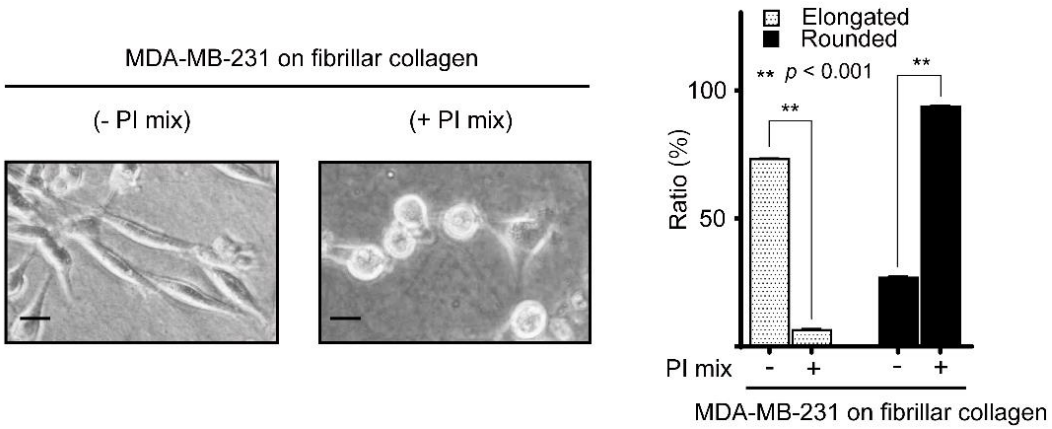

Figure 8-1. The morphological changes of MDA-MB-231 cells

Morphologies of MDA-MB-231cells on collagen seat were observed by phase contrast microscope (left). More than 300 cells were counted in each assay and the ratio of cells with an elongated or rounded shape are shown.

Arf6-AMAP1 pathway is involved in amoeboid-type invasion

In order to investigate the engagement of the Arf6-AMAP1 pathway in amoeboid-type invasion, the component proteins of this signalling was silenced by a short interference RNA (siRNA). LPA and EGF were used for the stimulation of GPCR and EGFR, respectively. Depletion of *GEP100*, *Arf6*, and *AMAP1* from MDA-MB-231 cells remarkably suppressed the amoeboid invasion (Fig. 8-2 and 8-4). These results strongly insist that the Arf6-AMAP1 pathway is thus essential for the amoeboid-type cell invasion.

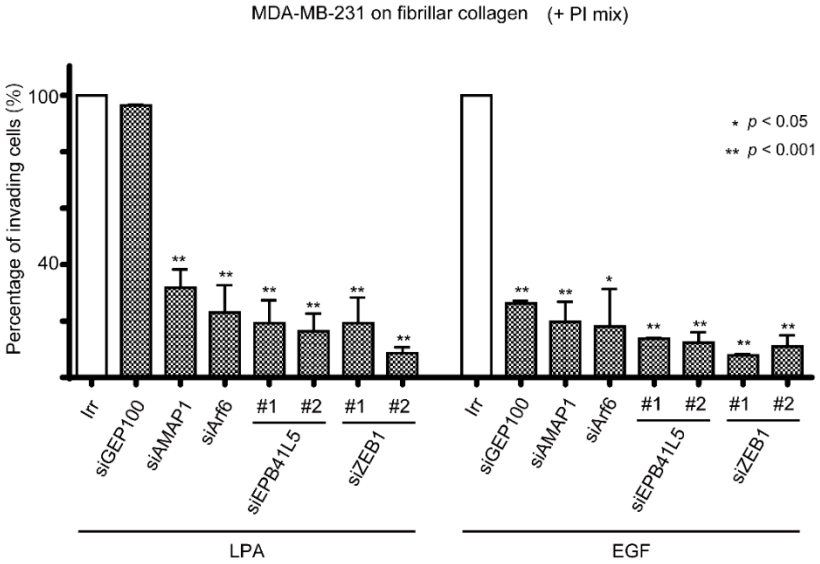

Figure 8-2. The amoeboid invasion activity

The percentages of cells pre-treated with each siRNAs which migrated through fibrillar collagen in the presence of PI mix were calculated.

ZEB1-EPB41L5 axis is required for amoeboid-type invasion

Considering that MDA-MB-231 has a mesenchymal feature, I hypothesized that the EMT programme might also be implicated in a protease-independent invasion. The downregulation by siRNA of *EPB41L5*, a mesenchymal specific protein, caused the reduction of amoeboid-type invasion (Fig. 8-2 and 8-4). To confirm this hypothesis, *ZEB1*, which is an EMT-related transcription factor and an inducer of the *EPB41L5* gene, was silenced. It was found that the knockdown of ZEB1 clearly blocked the invasion in the presence of PI mixed in both EGF and LPA stimulated MDA-MB-231 cells (Fig. 8-2). Therefore, these results demonstrated that the Arf6-based EMT programme is critical for driving the amoeboid-type cell invasion in response to the RTK and GPCR signalling.

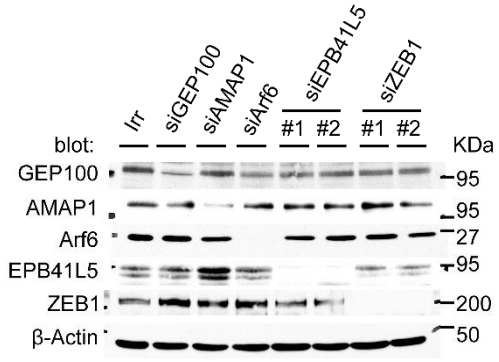

Figure 8-3. WB of silenced proteins
Immunoblotting of each protein that was silenced by indicated siRNA.

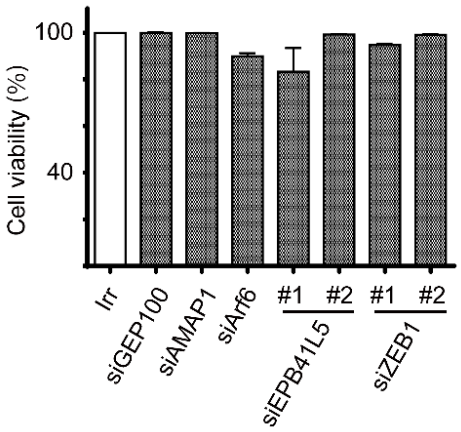

Figure 8-4. Cell viabilities
The viabilities of each gene-silenced cells in PI mix were measured.

8.3 Discussion

These results above, along with the reports in the literature, revealed a picture that the Arf6-pathway was stimulated either by the RTKs or LPA promoted mesenchymal-type and amoeboid-type invasion. Moreover, it has been demonstrated that the Arf6-based

mesenchymal programme is required for an amoeboid invasion. Therefore, an EMT-like change could be a prerequisite for both types of cell invasion. During the amoeboid invasion which was induced by protease inhibitors, the tumour cells are obliged to survive without integrin-ECM signalling, which is called anchorage-independent survival, or anoikis resistance. Indeed, in close relation with this, the EMT-like change during invasion is coupled with anoikis resistance to a certain extent. Our group has shown that EPB41L5 is also necessary for tumour metastasis (A. Hashimoto et al. 2016a, S. Hashimoto et al. 2016). Given the anoikis resistance might support cell survival during metastasis, it is reasonable to presume that EPB41L5 has a role in acquiring the resistance for anoikis. Molecular mechanisms, by which EPB41L5 functions in an amoeboid-type invasion as well as in a anoikis resistance, requires intense scrutiny.

9 Epithelial-specific histone modification of the *miR-96/182* locus targeting *AMAP1* mRNA predisposes p53 to suppress cell invasion in epithelial cells

9.1 Introduction

TP53 mutations often confer invasiveness to cancer cells, whilst fibroblasts show invasiveness in spite of possessing an intact *TP53*. As stated in chapter 6, AMAP1 is a key player in the Arf6-driven cell invasion. Sabe's group have already reported that in some malignant cancer cells that harbour mutant p53, there are high expression levels of AMAP1. I found that the AMAP1 levels under the control of p53 were not in fibroblasts but in epithelial cells, and this would address the molecular mechanism by which p53 has a epithelial-specific function in suppressing invasiveness via targeting AMAP1.

9.2 Results

AMAP1 expression is enhanced by *TP53* mutations in epithelial cells

In order to examine the levels of AMAP1 expression, I used MDA-MB-231 breast cancer cells and their two p53 derivatives that had been generated previously (Hashimoto et al. 2016b); endogenous p53 was silenced (shp53); shp53 cells expressing normal-p53 (shp53/wt cells). MDA-MB-231 parental cells exhibit higher invasiveness than shp53/wt cells (Hashimoto et al. 2016b), and AMAP1 protein and mRNA levels were largely reduced in the cells with normal-p53 (Fig. 9-1 and 9-2).

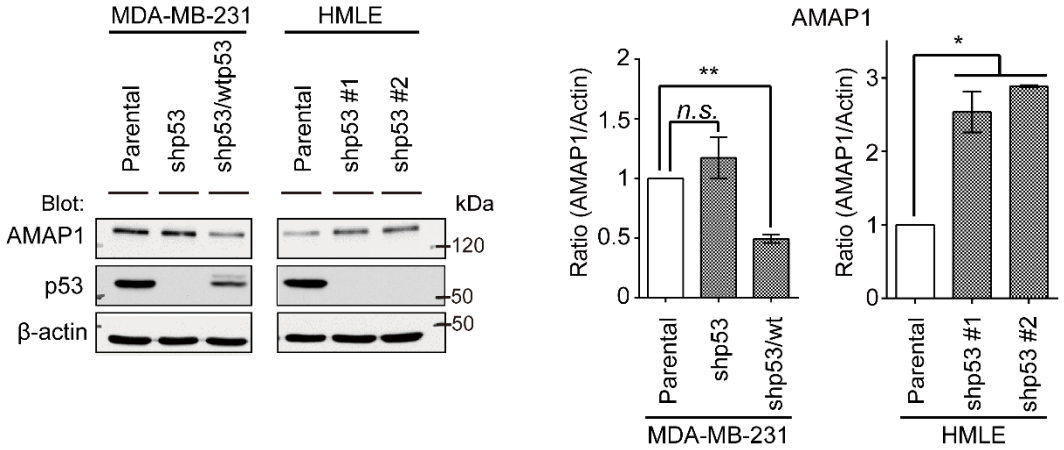

Figure 9-1. Protein levels of AMAP1

The AMAP1 and p53 expression levels by WB (left). Each density was measured by Image J and represented in the right graph.

To further investigate the generality of the p53 involvement in the suppression of AMAP1, I analysed non-transformed cells next. Primary normal mammary epithelial cells of humans were immortalized into HMLE cells (Elenbaas et al. 2001). Western-blotting showed that these HMLEs expressed the AMAP1 protein at a basal level and shRNA-mediated silencing of p53 in these cells significantly enhanced the AMAP1 expression, both at the protein and mRNA levels (Fig. 9-1 and 9-2). Therefore, these results insist that normal-p53 appeared to work on AMAP1 suppression in mammary epithelial cells, regardless of whether they are transformed or not.

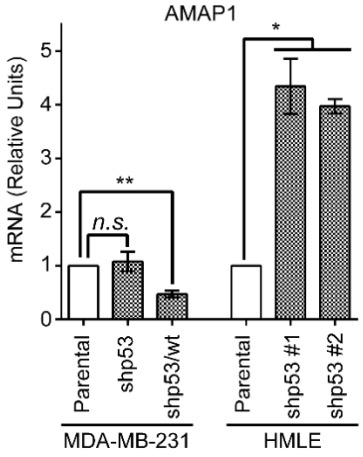

Figure 9-2. The level of AMAP1 mRNA.

N.s. stands for no significance. *: $P < 0.05$, **: $P < 0.01$

P53 induces miR-96 and miR-182 to target *AMAP1* mRNA

P53 controls the expression of various miRNAs (He et al. 2007). In order to understand the possible mechanisms that suppress the AMAP1 expression through normal-p53, I analysed the expression of miRNAs in MDA-MB-231 cells through the use of microarrays. In these experiments, I prepared miRNAs from cells cultured at sparse densities, because high densities could cause artefacts of miRNA preparation (N. G. Kim et al. 2011, Mori et al. 2014). Thirty-two miRNAs were found to be expressed at significantly higher levels in shp53/wt cells than in parental cells and shp53 cells (Fig. 9-3). By scanning these miRNA sequences, I picked out nine which have complementary sequences to the 3'-UTR of *AMAP1* mRNA (Fig. 9-4). In the TCGA RNASeq dataset on primary breast tumours in humans, miR-96 and miR-182 levels had a negative correlation with the level of *AMAP1* mRNA (Fig. 9-5). miR-96 and miR-182 are members of the miR-183-96-182 cluster (Ma et al. 2016), and it was shown previously that p53 was responsible for the expression of this cluster by binding directly to its promoter (Kouri et al. 2015).

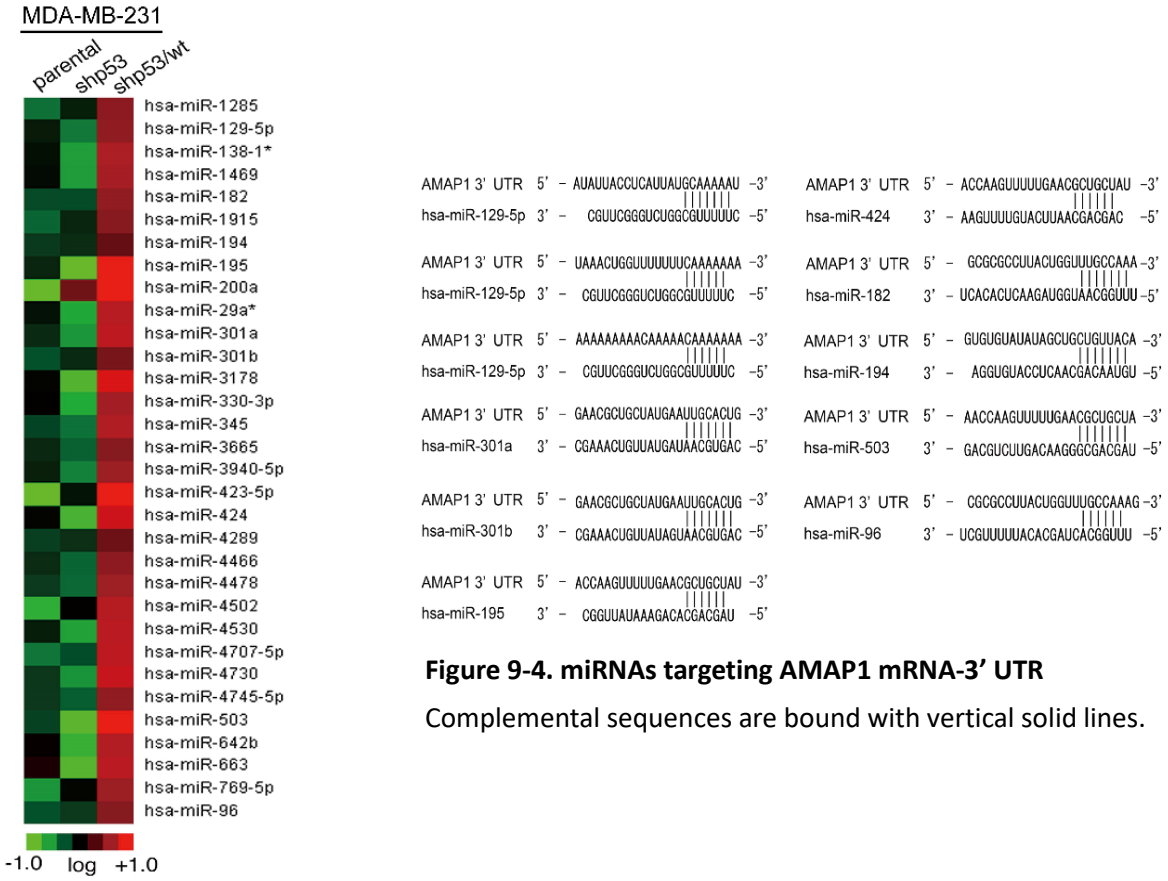

Figure 9-4. miRNAs targeting AMAP1 mRNA-3' UTR

Complemental sequences are bound with vertical solid lines.

Figure 9-3. Heatmap of miRNA expression

Colour scale is modified for log 2.

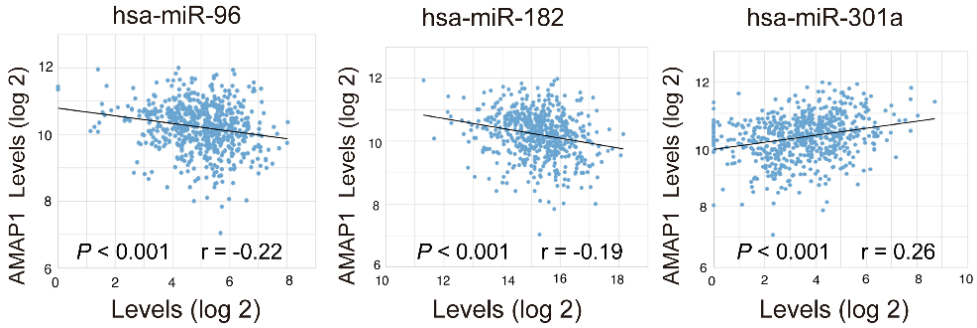

Figure 9-5. Correlation diagrams between AMAP1 and each miRNA

Pearson correlation coefficients (*r*) were calculated.

By using a luciferase reporter assay in a reconstituted system using HEK293T cells, I confirmed that these two miRNAs were bound to the 3'-UTR of *AMAP1* mRNA. I generated a reporter gene, in which the firefly luciferase gene was fused to the *AMAP1* 3'-UTR or the mutated *AMAP1* 3'-UTR, and found that both miR-96 and miR-182 have the ability to target this 3'-UTR (Fig. 9-6). As a negative control, I then analysed the miR-301a, which was induced by intact p53 and had a sequence complementary to the *AMAP1* 3'-UTR but had no negative correlation between this miRNA and *AMAP1* mRNA (Fig. 9-5) in the TCGA database. Furthermore, I found that the miR-301a is incapable of targeting the *AMAP1* 3'-UTR in the reconstitution system (Fig. 9-6).

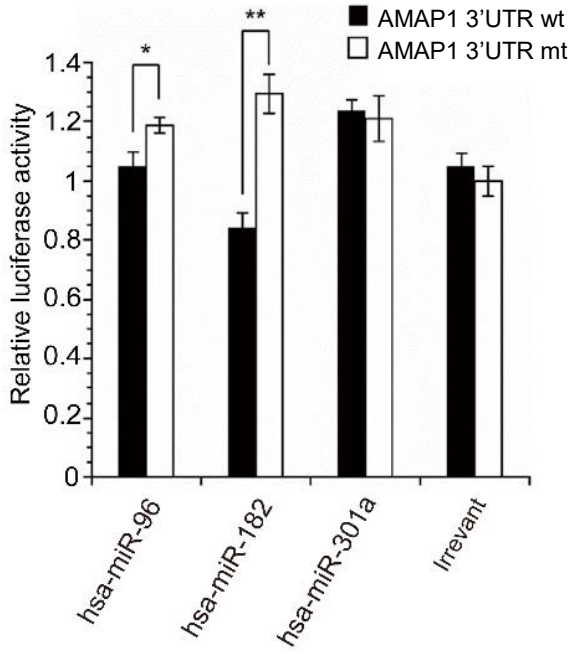

Figure 9-6. The capacity of targeting AMAP1
The interactions among AMAP1 mRNA 3'UTR (wt) or its mutant (mt), and each miRNAs were assessed by dual-luciferase assay.

The suppression of miR-96 and miR-182 expression upon the loss of normal p53 was also observed in the HMLE cells (Fig. 9-7), and I confirmed statistically significant changes to be present in *miR-96* and *miR-182* expression levels in MDA-MB-231 cells, depending on the p53 status (Fig. 9-7). Therefore, miR-96 and miR-182 are likely to be implicated in the under-expression of *AMAP1* mRNA in response to the intact-p53.

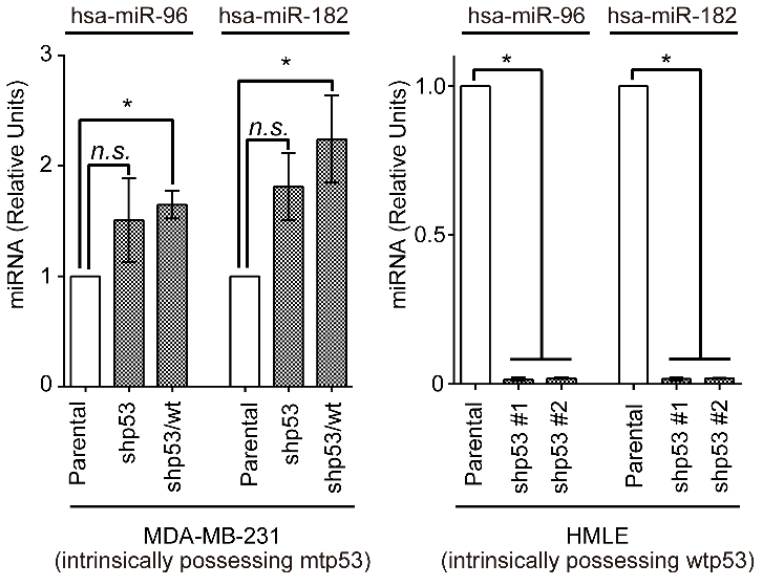

Figure 9-7. The levels of miRNAs among each cell.
The expression levels of two miRNA candidates were assessed in each cell indicated above.

The p53-*miR-96*/*182* axis is specific to epithelial cells, not in fibroblasts

This led me to ponder as to whether this particular p53-miR-96/182 axis is utilised in various types of cells. The MCF7 breast cancer cells expresses a wild-type p53 and their invasiveness is low (Wang et al. 2009). Consequently, both AMAP1 protein and AMAP1 mRNA are weakly expressed in MCF7 cells at much lower levels than the MDA-MB-231 cells (Fig. 9-8). On the other hand, normal human fibroblasts bearing normal *TP53*, such as BJ cells, expressed AMAP1 protein and mRNA at higher levels than MCF7 cells (Fig. 9-8). Surprisingly, BJ cells were not seen to remarkably express miR-96 and miR-182 (Fig. 9-8).

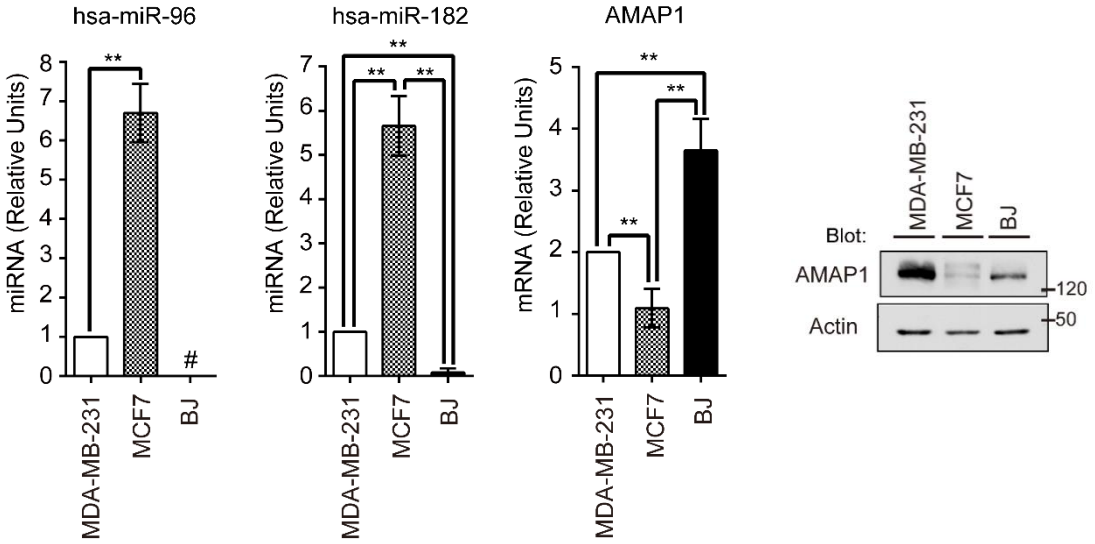

Figure 9-8. AMAP1 and miRNAs expression levels

The expression levels of AMAP1 mRNA and protein were assessed by qPCR and WB, respectively. The levels of miR-96 and miR-182 were also measured by qPCR among MDA-MB-231, MCF7 and BJ cells.

As such, p53 mainly function as a transcription factor. I thus examined the promoter status of miR-183/96/182 cluster by the ENCODE dataset, and the data indicated that H3K27 trimethylation (H3K27me3) histone modification was enriched around the promoter region of the *miR-183-96-182* cistron in fibroblasts, as well as in other non-epithelial cells, whereas this locus was enriched with H3K27 acetylation (H3K27ac) in epithelial cells (Fig. 9-9). This data suggested that the transcription of this cluster appeared to be epigenetically suppressed in fibroblasts, although it can be transcribed within epithelial cells.

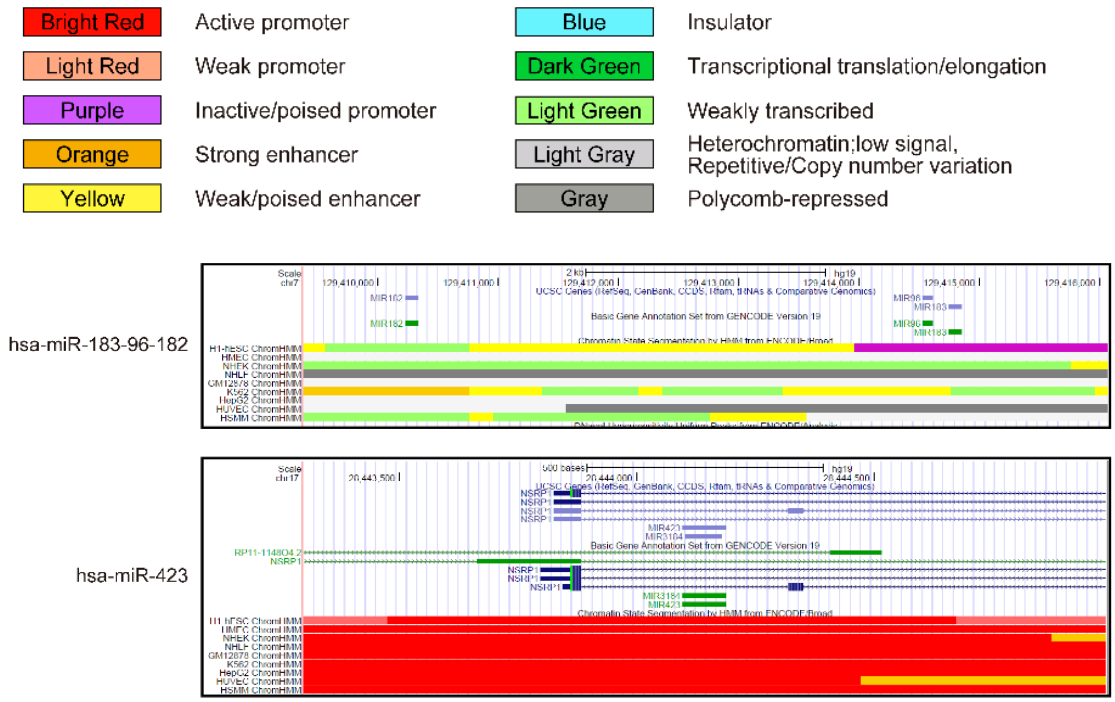

Figure 9-9. The ENCODE data of miRNAs

The ENCODE data of miR-183-96-182 and miR-423 loci are shown by UCSC Genome Browser. The definitions of the colours are indicated above. hESC: human embryonic stem cells, HMEC: human mammary epithelial cells, NHEK: normal human epidermal keratinocytes, NHLF: normal human lung fibroblasts, GM12878: B-lymphocyte transformed by Epstein-Barr virus, K562: highly undifferentiated and granurocytic myelogenous leukemia cells, HepG2: hephepatocytellular carcinoma cells, HUVEC: human umbilical vein endothelial cells, HSMM: human skeletal muscle myoblasts.

Not all p53-miRNA axes are specific to epithelial cells

The results above indicate an epithelial specificity of the p53-miR-96/182 axis. Normal p53 is known to induce different kinds of miRNAs, as I have shown above (see Fig.9-4). My final interest is therefore in understanding whether the induction of miRNAs by p53 is specific to epithelial cells and not occurring within fibroblasts. In the MDA-MB-231 cells, the *miR-423* is highly induced in the presence of normal p53, but does not have complementary sequences to the *AMAP1* mRNA 3'-UTR (Fig. 9-3). I found that histone modification of the *miR-423* locus was similar both in epithelial cells and fibroblasts and was categorized as an active promoter (Fig. 9-9). In the same way, the gene loci of other

miRNAs were controlled by normal-p53 in MDA-MB-231 cells, and were not necessarily suppressed in fibroblasts. Thus, this data led to the conclusion that not all p53-miRNA axes are specific to epithelial cells.

9.3 Discussion

In this study, I demonstrated that AMAP1 mRNA levels were restricted by normal-p53 in epithelial cells, but not in fibroblasts (Fig. 9-10). *AMAP1* mRNA contains a 5'-TOP-like sequence, and is hence under the control of the mTORC1 (submitted elswhere). As such, epithelial cells appear to have a double safeguard system where high expression of AMAP1 is suppressed by targeting the 5'-UTR and 3'-UTR of *AMAP1* mRNA, in order to prevent the cell-invasive phenotype from readily appearing. In other words, normal-p53 might be an epithelial-specific guardian aimed at preventing cell invasiveness, under conditions where mTORC1 is activated such as during active cell proliferation.

As described in Chapter 6, the basic functions of miRNAs are to coordinate the expression levels of various mRNA sets required in specific cellular functions. To be consistent, the miR-96 can target Foxf2 and Ezrin mRNAs to prevent cell invasion in lung cancers and renal cancers (Kundu et al. 2016, Yu et al. 2015) . In other reports, miR-183 is involved in the inhibition of the invasion and metastasis of different cancers, such as the lung, breast, and osteosarcoma (Lowery et al. 2010, Wang et al. 2008, Zhu et al. 2012). Taking into consideration that the normal-p53 can induce miR-200c against EMT progression in HMECs and MCF12A, p53 appears to have various means of suppressing the invasiveness (Chang et al. 2011).

My data indicates that p53 indubitably important for maintaining the innate statuses of diverse cell linages, but has the slightest function in deciding cell fate. Thus, these results give rise to the following questions: 1) What determines (and when) the epigenetic

regulation of certain miRNAs to render p53 with the ability to prevent invasiveness in epithelial cells; and 2) How non-epithelial cells increase *AMAP1* mRNA levels in the presence of an intact-p53 to gain high invasiveness.

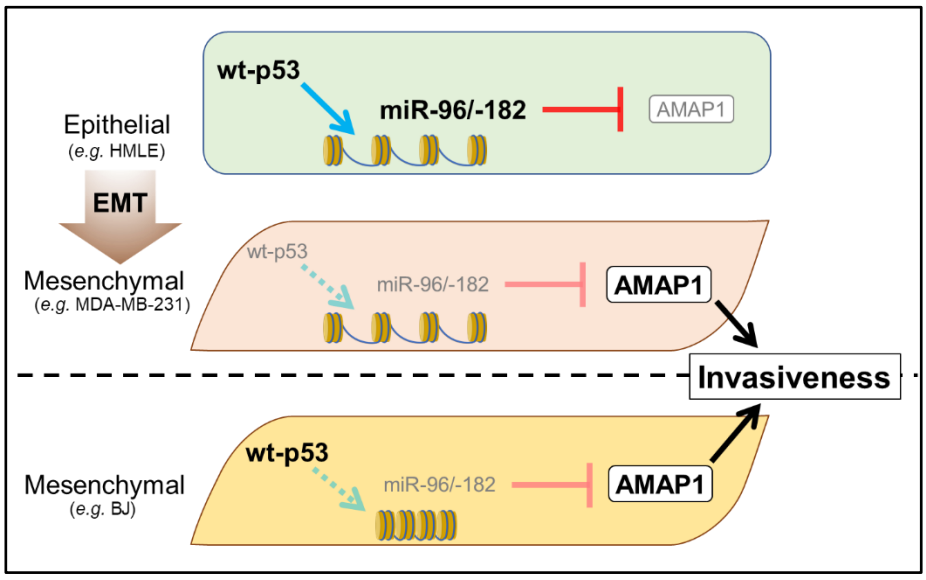

Figure 9-10. The graphical explanation of p53-miR-96/-182 axis

In epithelial cells p53 can access miRNA-96/-182 loci, thus the loss of p53 causes AMAP1 enhancement through the decrease of miRNAs. On the other hand, the *bona fide* mesenchymal cells p53 cannot access that locus. AMAP1 is expressed through other mechanisms.

10 Epithelial-mesenchymal transition accompanies mitochondrial fission and enhanced OXPHOS activity

10.1 Introduction

As mentioned in chapter 6, EMT is essential for tumour malignancy, including its metastatic ability, anoikis resistance, chemoresistance, and radiotherapy resistance. Cells exposed to severe stress can reprogram their internal condition, especially metabolic system, either for their survival or to commit suicide, which is called apoptosis. Malignant cancer cells are the chosen population which was obliged to survive in harsh condition, such as chemotherapy and radiation, and almost all of them presumably underwent EMT. Consequently, I investigated a molecular mechanism that underlies metabolic regulation and EMT by mainly focusing on mitochondria bioenergetics and dynamism during EMT. It has already demonstrated by Dr Otsuka in Sabe's laboratory that the mitochondria of both normal and transformed cell lines tend to divide during EMT. Moreover, normal cells have enhanced OXPHOS capacity during EMT. However, certain issues remain and need further clarification, such as how cells perform this mitochondria fission and the enhancement of OXPHOS, whether these mitochondria dynamics and OXPHOS are coupled, the molecular mechanism of this phenomenon, along with the biological question on mitochondria during EMT.

10.2 Results

Enhancement of OXPHOS capacity in normal cells occurs during EMT

It is generally accepted that mitochondria fusion might have a general role in enhancing

OXPHOS activity. Consequently, mitochondria fission may impair OXPHOS activity. In order to assess OXPHOS capacity in these two cell lines, we measured OCR consumption as a surrogate of ATP production. Interestingly, the OCR of NMuMG cells were enhanced two days from EMT induction, whilst that of the A549 was not altered (Fig. 10-1). These results, especially in non-transformed cells, indicate that mitochondrial fission does not necessarily impair OXPHOS activity.

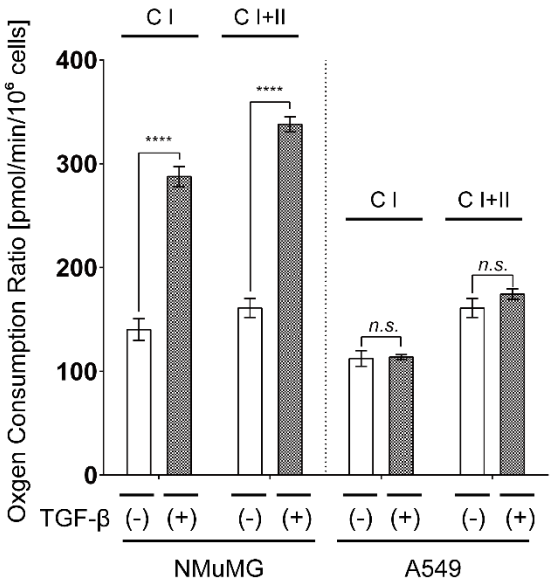

Figure 10-1. Oxygen consumption ratio among NMuMG and A549 cells
NMuMG: normal murine mammary epithelial cells, A549: lung adenocarcinoma. C I: complex I, C II: complex I + II.
****: $P < 0.0001$, $n < 3$. *n.s.* means no significance. ANOVA test was used.

mitoNEET is downregulated during EMT

In order to investigate a molecular mechanism, I searched gene expression data from Gene Expression Omnibus, and found datasets of NMuMG cells that were stimulated either with or without TGF-beta (table). The genes which work in mitochondria were picked up. In the list, I targeted the mitoNEET/Cisd1, which exists in the outer mitochondrial membrane and whose function has remained almost unknown. As expected, the expression levels of mitoNEET mRNA and protein were downregulated after EMT induction (Fig. 10-2 and 10-3). In order to examine whether this suppression is a general

event, the levels of mitoNEET were assessed among the various cancer cell lines (Fig. 10-3). This data thus suggests that mitoNEET could be downregulated in mesenchymal cells.

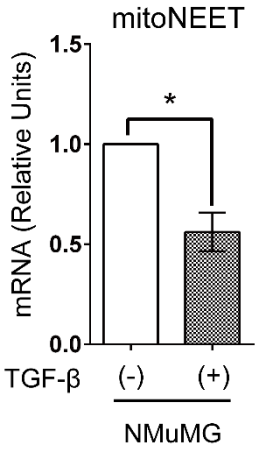

Figure 10-2. Quantification of mRNA levels of mitoNEET
mitoNEET of NMuMG cells with or without TGF-beta were quantified by qRT-PCR. n < 3. *: $P < 0.05$.

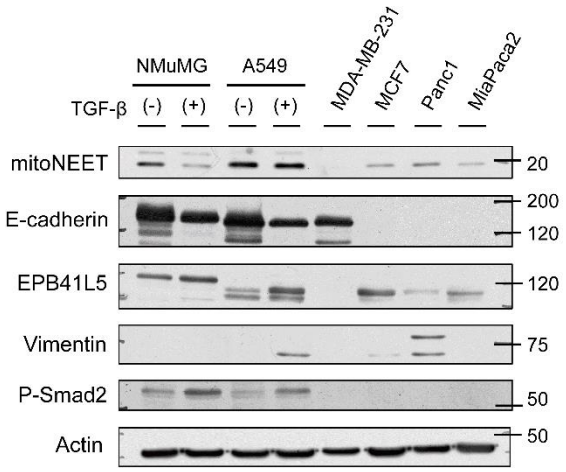

Figure 10-3. Immunoblotting among various cells
The expression levels of mitoNEET was assessed among different types of cells. P-smad2: phosphorylated smad2.

The downregulation of mitoNEET is sufficient for the enhancement of OXPHOS during EMT

To further investigate the role of mitoNEET, mitoNEET was overexpressed in NMuMG cells (Fig.10-4). Surprisingly, the overexpression of mitoNEET did not impair the capacity of OXPHOS. Rather, it repressed the augment of OXPHOS during EMT. Conversely, silencing mitoNEET in a steady state did not affect the OCR (Fig.10-5).

These results indicate that the reduction of mitoNEET protein is sufficient for enhancing OXPHOS.

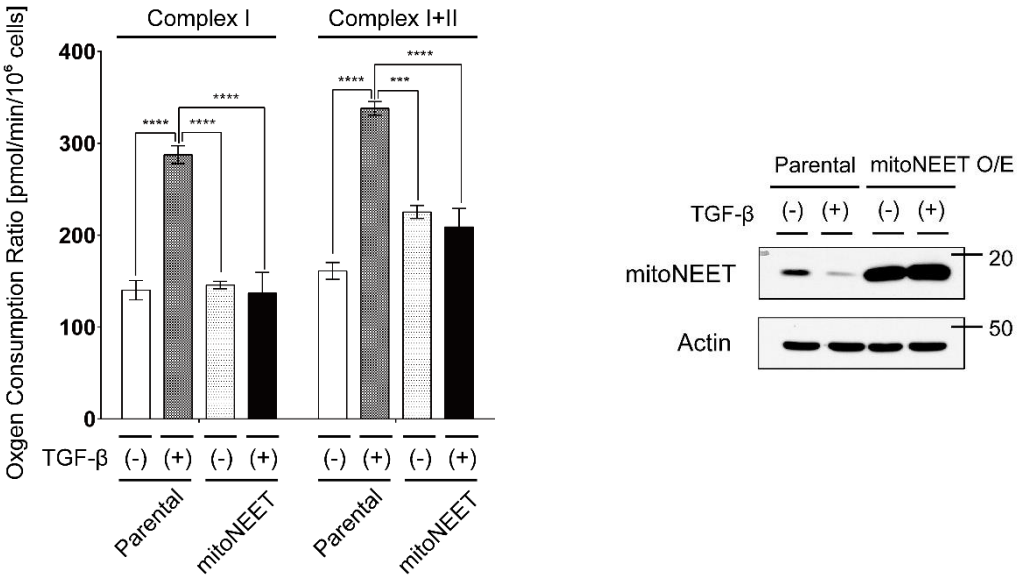

Figure 10-4. Oxygen consumption rate among parental cells and mitoNEET overexpressing cells
2 days after TGF-b stimulation, their OCR was measured by O2k. ***: $P < 0.005$, ****: $P < 0.0001$ ANOVA test was used. Immunoblotting for checking mitoNEET overexpression (right).

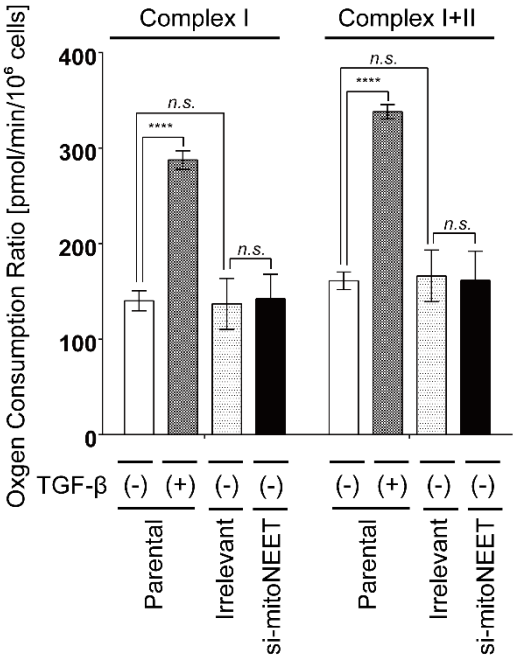

Figure 10-5. Oxygen consumption rate among parental cells and mitoNEET silenced cells
2 days after TGF-b stimulation, their OCR was measured by O2k. ***: P < 0.005, ****: P < 0.0001. ANOVA test was used.

10.3 **Discussion**

In these experiments, the measurement of OCR by Oxy2k is a surrogate for OXPHOS and actually reflects the capacity of OXPHOS. To measure the real activity of OXPHOS *in situ*, an ATP sensor (GOATeam2) should be used.

Mitochondria dynamics and bioenergetics have been thought to have an intimate relationship. However, the data shown here suggests that this relationship might not always be interconnected. To confirm this suggestion, an examination is required as to whether manipulation of key proteins that regulate mitochondria dynamics, such as Drp1, Mfn1/2, and opa1, affects mitochondria OXPHOS during EMT.

My results also give rise to several questions, such as 1) What is a molecular mechanism of the enhancement of OXPHOS; 2) What is the biological meaning underlying this phenomenon; during EMT. One possible answer against the former question would be that motility as the result of EMT needs more energy, namely ATP, because actin remodelling at the leading edge would consume a large amount of ATPs.

This theme is still in its infancy, and thus further investigation should be done.

11 General Discussion

The aim of this project was to elucidate the entity of EMT, especially in cancer. EMT is a dynamic process that requires cytoskeletal, epigenetic, and metabolic remodelling for epithelial cells to obtain mesenchymal function including anoikis resistance and motility. A substantial amount of evidence has also been provided to show that EMT is a fundamental process for malignant progression, such as cancer stemness, treatment-resistance and immune evasion. Therefore, it is important to pile up the knowledge on EMT, which could then be used to improve contemporary therapy.

This body of work aimed to investigate characteristics of EMT through three approaches; (1) to clarify the role of Arf6-AMAP1-EPB41L5 pathway on amoeboid invasion; (2) to evaluate the epigenetic alterations of AMAP1 expression between EMT-cells and *bona fide* mesenchymal cells; (3) to determine a molecular mechanism by which cells can manage to meet the energetic requirement during EMT.

Mesenchymal cells mainly move in the way that is based on focal adhesion and integrin recycling with a secretion of matrix-metalloproteinases for a degradation of the extracellular matrix. However, clinical trials that targeted this characteristic brought negative outcomes. This was attributed to the lack of knowledge that tumour cells have the alternative of mesenchymal invasion or amoeboid invasion. With regards to mesenchymal invasion, our group has exhibited a series of evidence that various malignant cancer cells, including breast, lung, head and neck, and renal cancer can exploit the Arf6-AMAP1 pathway for their invasiveness. Arf6 is renowned for its role in regulating endocytic trafficking and actin cytoskeleton dynamics. Recently, our studies have demonstrated that the mevalonate pathway (MVP) enhances Arf6 signalling by

promoting the prenylation and membrane trafficking activity of Rab11b (A. Hashimoto et al. 2016b). It has also been reported that the efficacies of statins and gemcitabine can be augmented through silencing the geranylgeranyl transferase-II (GGT-II), which is essential for the functionalising of Rab11b, or EPB41L5. In this thesis, I have shown that the Arf6-AMAP1 pathway is exploited for amoeboid invasion (Chapter 8). Therefore, combination chemotherapy with statins would be immensely promising.

These strategies that include the use of statins are not omnipotent, since the abnormal overexpression of every component of the Arf6 pathway is sufficient for statin treatments. The second approach mentioned above was to focus on the epigenetic status that allows invasive cells to overexpress AMAP1. p53 mutation (i.e., loss of normal-p53) has been reported to play a critical role in evoking EMT through a suppression of certain miRNAs. Our group has reported that the p53-miRNA axis alone is not enough to explain the epithelia's integrity. To provide details, there are two types of manners to maintain epithelial integrity; p53-dependent or independent manners. In a p53-dependent manner, p53 can bind the locus of the epithelial-specific gene (e.g., E-cadherin) and then antagonize the influence of EZH2, which is a major histone methyl transferase for EMT (Oikawa et al. 2018). These results are closely related to the picture portrayed in this thesis (Chapter 9), where it shows that p53 is just a pawn, not a king, in deciding the cell destiny. From these results arise the most profound questions as to when and how the cell destiny would be made.

Prior to various cellular functions during and after EMT, cells must generate or extract energy. Indeed, disturbance of the metabolism can wreak havoc on life itself, and the requirement can be different among cell types (i.e., mesenchymal, epithelial, endothelial,

neuronal and *etc*.). This thesis has shown that normal epithelial cells enhance their OXPHOS capacity during EMT with fissions of mitochondria. It is thus worthwhile for further investigation as there might be different mechanisms and entities compared to T lymphocyte in which mitochondria are fragmented for the promotion of aerobic glycolysis.

All the findings that have been demonstrated in this thesis could have the potential to usher in a new age of cancer biology, and this knowledge, once harnessed, could lead to advancements in cancer therapy, thereby contributing to society as a whole.

12 Acknowledgements

I would like to thank my supervisor, Professor Hisataka Sabe, for introducing me to leading-edge biomedical research, and guiding me with insightful advice and knowledge on what makes good research activity, all while providing opportunities to share and discuss ideas and research with both domestic and international communities.

I am also grateful to the laboratory staffs, Dr Tsukasa Oikawa, Dr Yasuhito Onodera, Dr Ari Hashimoto, and Dr Shigeru Hashimoto, who was one of the members and is an associate professor in Osaka University now, for their warm-hearted and perceptive guidance on my research.

I am really obliged to Dr Shingo Takada for his kind collaboration.

I greatly appreciate my senior, Dr Yutaro Otsuka, my junior, Mr Kiyoshi Fukunaga, Ms Mei Horikawa, Ms Shion Kachi, and Mr Soichiro Hata for their inspiring discussion, along with Ms Ayae Oda for her secretarial work.

I would like to show my sincere appreciation to The Takeda Science Foundation for their financial support during the tenure of my PhD programme.

Last but not least, I would like to express my gratitude, from the bottom of my heart, to my family and friends for giving me the motivation to complete my PhD. This would be particularly to my parents, for all their dedication and continuous support.

13 References

Akagi, T., Sasai, K. and Hanafusa, H. (2003) Refractory nature of normal human diploid fibroblasts with respect to oncogene-mediated transformation. *Proc Natl Acad Sci U S A, 100*(23), pp. 13567-72.

Cancer Research UK, https://www.cancerresearchuk.org/health-professional/cancer-statistics/worldwide-cancer, Accessed [11] [2018].

Chan, D. C. (2012) Fusion and fission: interlinked processes critical for mitochondrial health. *Annu Rev Genet, 46*, pp. 265-87.

Chang, C. J., Chao, C. H., Xia, W., Yang, J. Y., Xiong, Y., Li, C. W., Yu, W. H., Rehman, S. K., Hsu, J. L., Lee, H. H., et al. (2011) p53 regulates epithelial-mesenchymal transition and stem cell properties through modulating miRNAs. *Nat Cell Biol, 13*(3), pp. 317-23.

Coussens, L. M., Fingleton, B. and Matrisian, L. M. (2002) Matrix Metalloproteinase Inhibitors and Cancer—Trials and Tribulations. *Science, 295*(5564), pp. 2387-2392.

Dambal, S., Shah, M., Mihelich, B. and Nonn, L. (2015) The microRNA-183 cluster: the family that plays together stays together. *Nucleic Acids Res, 43*(15), pp. 7173-88.

Donaldson, J. G. and Jackson, C. L. (2011) ARF family G proteins and their regulators: roles in membrane transport, development and disease. *Nat Rev Mol Cell Biol, 12*(6), pp. 362-75.

Elenbaas, B., Spirio, L., Koerner, F., Fleming, M. D., Zimonjic, D. B., Donaher, J. L., Popescu, N. C., Hahn, W. C. and Weinberg, R. A. (2001) Human breast cancer cells generated by oncogenic transformation of primary mammary epithelial cells. *Genes Dev, 15*(1), pp. 50-65.

Fischer, K. R., Durrans, A., Lee, S., Sheng, J., Li, F., Wong, S. T., Choi, H., El Rayes, T., Ryu, S., Troeger, J., et al. (2015) Epithelial-to-mesenchymal transition is not required for lung metastasis but contributes to chemoresistance. *Nature,*

527(7579), pp. 472-6.

Friedl, P. and Wolf, K. (2003) Tumour-cell invasion and migration: diversity and escape mechanisms. *Nature Reviews Cancer, 3*, pp. 362.

Gebert, L. F. R. and MacRae, I. J. (2018) Regulation of microRNA function in animals. *Nature Reviews Molecular Cell Biology*.

Hashimoto, A., Hashimoto, S., Sugino, H., Yoshikawa, A., Onodera, Y., Handa, H., Oikawa, T. and Sabe, H. (2016a) ZEB1 induces EPB41L5 in the cancer mesenchymal program that drives ARF6-based invasion, metastasis and drug resistance. *Oncogenesis, 5*(9), pp. e259.

Hashimoto, A., Oikawa, T., Hashimoto, S., Sugino, H., Yoshikawa, A., Otsuka, Y., Handa, H., Onodera, Y., Nam, J. M., Oneyama, C., et al. (2016b) P53- and mevalonate pathway-driven malignancies require Arf6 for metastasis and drug resistance. *J Cell Biol, 213*(1), pp. 81-95.

Hashimoto, S., Mikami, S., Sugino, H., Yoshikawa, A., Hashimoto, A., Onodera, Y., Furukawa, S., Handa, H., Oikawa, T., Okada, Y., et al. (2016) Lysophosphatidic acid activates Arf6 to promote the mesenchymal malignancy of renal cancer. *Nat Commun, 7*, pp. 10656.

Hay, E. D. (1968) Organization and fine structure of epithelium and mesenchyme in the developing chick embryo. pp. Proceedings of the 18th Hahnemann Symposium: 31-55.

He, L., He, X., Lim, L. P., de Stanchina, E., Xuan, Z., Liang, Y., Xue, W., Zender, L., Magnus, J., Ridzon, D., et al. (2007) A microRNA component of the p53 tumour suppressor network. *Nature, 447*(7148), pp. 1130-4.

Hirano, M., Hashimoto, S., Yonemura, S., Sabe, H. and Aizawa, S. (2008) EPB41L5 functions to post-transcriptionally regulate cadherin and integrin during epithelial-mesenchymal transition. *J Cell Biol, 182*(6), pp. 1217-30.

Kastenhuber, E. R. and Lowe, S. W. (2017) Putting p53 in Context. *Cell, 170*(6), pp. 1062-1078.

Kielkopf, L. C., Bauer, W. and Urbatsch, L. I. (2012). Expressing Cloned Genes for Protein Production, Purification, and Analysis. In Molecular cloning : a laboratory manual, Fourth edition, Green, R. M. and Sambrook, J., Cold Spring Harbor, N.Y. : Cold Spring Harbor Laboratory Press, pp. 1599-1608.

Kim, N. G., Koh, E., Chen, X. and Gumbiner, B. M. (2011) E-cadherin mediates contact inhibition of proliferation through Hippo signaling-pathway components. *Proc Natl Acad Sci U S A, 108*(29), pp. 11930-5.

Kim, T., Veronese, A., Pichiorri, F., Lee, T. J., Jeon, Y.-J., Volinia, S., Pineau, P., Marchio, A., Palatini, J., Suh, S.-S., et al. (2011) p53 regulates epithelial–mesenchymal transition through microRNAs targeting ZEB1 and ZEB2. *J Exp Med, 208*(5), pp. 875-883.

Kinoshita, R., Nam, J. M., Ito, Y. M., Hatanaka, K. C., Hashimoto, A., Handa, H., Otsuka, Y., Hashimoto, S., Onodera, Y., Hosoda, M., et al. (2013) Co-overexpression of GEP100 and AMAP1 proteins correlates with rapid local recurrence after breast conservative therapy. *PLoS One, 8*(10), pp. e76791.

Kouri, F. M., Hurley, L. A., Daniel, W. L., Day, E. S., Hua, Y., Hao, L., Peng, C.-Y., Merkel, T. J., Queisser, M. A., Ritner, C., et al. (2015) miR-182 integrates apoptosis, growth, and differentiation programs in glioblastoma. *Genes Dev, 29*(7), pp. 732-745.

Kruiswijk, F., Labuschagne, C. F. and Vousden, K. H. (2015) p53 in survival, death and metabolic health: a lifeguard with a licence to kill. *Nat Rev Mol Cell Biol, 16*(7), pp. 393-405.

Kundu, S. T., Byers, L. A., Peng, D. H., Roybal, J. D., Diao, L., Wang, J., Tong, P., Creighton, C. J. and Gibbons, D. L. (2016) The miR-200 family and the miR-183~96~182 cluster target Foxf2 to inhibit invasion and metastasis in lung cancers. *Oncogene, 35*(2), pp. 173-86.

Lambert, A. W., Pattabiraman, D. R. and Weinberg, R. A. (2017) Emerging Biological Principles of Metastasis. *Cell, 168*(4), pp. 670-691.

Lamouille, S., Xu, J. and Derynck, R. (2014) Molecular mechanisms of epithelial-

mesenchymal transition. *Nat Rev Mol Cell Biol, 15*(3), pp. 178-96.

Li, Y. and Kowdley, K. V. (2012) MicroRNAs in Common Human Diseases. *Genomics, Proteomics & Bioinformatics, 10*(5), pp. 246-253.

Lowery, A. J., Miller, N., Dwyer, R. M. and Kerin, M. J. (2010) Dysregulated miR-183 inhibits migration in breast cancer cells. *BMC Cancer, 10*, pp. 502-502.

Ma, Y., Liang, A. J., Fan, Y. P., Huang, Y. R., Zhao, X. M., Sun, Y. and Chen, X. F. (2016) Dysregulation and functional roles of miR-183-96-182 cluster in cancer cell proliferation, invasion and metastasis. *Oncotarget, 7*(27), pp. 42805-42825.

Mani, S. A., Guo, W., Liao, M.-J., Eaton, E. N., Ayyanan, A., Zhou, A. Y., Brooks, M., Reinhard, F., Zhang, C. C., Shipitsin, M., et al. (2008) The Epithelial-Mesenchymal Transition Generates Cells with Properties of Stem Cells. *Cell, 133*(4), pp. 704-715.

Menju, T., Hashimoto, S., Hashimoto, A., Otsuka, Y., Handa, H., Ogawa, E., Toda, Y., Wada, H., Date, H. and Sabe, H. (2011) Engagement of overexpressed Her2 with GEP100 induces autonomous invasive activities and provides a biomarker for metastases of lung adenocarcinoma. *PLoS One, 6*(9), pp. e25301.

Mizuno, H., Spike, B. T., Wahl, G. M. and Levine, A. J. (2010) Inactivation of p53 in breast cancers correlates with stem cell transcriptional signatures. *Proceedings of the National Academy of Sciences, 107*(52), pp. 22745-22750.

Mori, M., Triboulet, R., Mohseni, M., Schlegelmilch, K., Shrestha, K., Camargo, F. D. and Gregory, R. I. (2014) Hippo signaling regulates microprocessor and links cell-density-dependent miRNA biogenesis to cancer. *Cell, 156*(5), pp. 893-906.

Morishige, M., Hashimoto, S., Ogawa, E., Toda, Y., Kotani, H., Hirose, M., Wei, S., Hashimoto, A., Yamada, A., Yano, H., et al. (2008) GEP100 links epidermal growth factor receptor signalling to Arf6 activation to induce breast cancer invasion. *Nat Cell Biol, 10*(1), pp. 85-92.

Muller, P. A. J., Caswell, P. T., Doyle, B., Iwanicki, M. P., Tan, E. H., Karim, S., Lukashchuk, N., Gillespie, D. A., Ludwig, R. L., Gosselin, P., et al. (2009) Mutant

p53 Drives Invasion by Promoting Integrin Recycling. *Cell, 139*(7), pp. 1327-1341.

Nieto, M. A., Huang, Ruby Y.-J., Jackson, Rebecca A. and Thiery, Jean P. (2016) EMT: 2016. *Cell, 166*(1), pp. 21-45.

O. Warburg, F. D., B. Kaiser (1931) The metabolism of tumours. Investigations from the Kaiser-Wilhelm Institute for Biology, Berlin-Dahlem. Edited by Otto Warburg, Kaiser-Wilhelm Institute for Biology, Berlin-Dahlem. Translated from the German edition, with accounts of additional recent researches, by Frank Dickens, M.A., Ph.D., whole-time worker for the Medical Research Council, Courtauld Institute of Biochemistry, Middlesex Hospital, London. Demy 8vo. Pp. 327 + xxix. Illustrated. 1930. London: Constable & Co. Ltd. 40s. net. *BJS, 19*(73), pp. 168-168.

Oikawa, T., Otsuka, Y., Onodera, Y., Horikawa, M., Handa, H., Hashimoto, S., Suzuki, Y. and Sabe, H. (2018) Necessity of p53-binding to the CDH1 locus for its expression defines two epithelial cell types differing in their integrity. *Sci Rep, 8*(1), pp. 1595.

Onodera, Y., Nam, J. M., Hashimoto, A., Norman, J. C., Shirato, H., Hashimoto, S. and Sabe, H. (2012) Rab5c promotes AMAP1-PRKD2 complex formation to enhance beta1 integrin recycling in EGF-induced cancer invasion. *J Cell Biol, 197*(7), pp. 983-96.

Onodera, Y., Nam, J. M., Horikawa, M., Shirato, H. and Sabe, H. (2018) Arf6-driven cell invasion is intrinsically linked to TRAK1-mediated mitochondrial anterograde trafficking to avoid oxidative catastrophe. *Nat Commun, 9*(1), pp. 2682.

Onodera, Y., Nam, J. M. and Sabe, H. (2013) Intracellular trafficking of integrins in cancer cells. *Pharmacol Ther, 140*(1), pp. 1-9.

Otsuka, Y., Sato, H., Oikawa, T., Onodera, Y., Nam, J. M., Hashimoto, A., Fukunaga, K., Hatanaka, K. C., Hatanaka, Y., Matsuno, Y., et al. (2016) High expression of EPB41L5, an integral component of the Arf6-driven mesenchymal program, correlates with poor prognosis of squamous cell carcinoma of the tongue. *Cell Commun Signal, 14*(1), pp. 28.

Peng, Y. and Croce, C. M. (2016) The role of MicroRNAs in human cancer. *Signal Transduct Target Ther, 1*, pp. 15004.

Rinon, A., Molchadsky, A., Nathan, E., Yovel, G., Rotter, V., Sarig, R. and Tzahor, E. (2011) p53 coordinates cranial neural crest cell growth and epithelial-mesenchymal transition/delamination processes. *Development, 138*(9), pp. 1827-1838.

Sabe, H., Hashimoto, S., Morishige, M., Ogawa, E., Hashimoto, A., Nam, J.-M., Miura, K., Yano, H. and Onodera, Y. (2009) The EGFR-GEP100-Arf6-AMAP1 Signaling Pathway Specific to Breast Cancer Invasion and Metastasis(†). *Traffic (Copenhagen, Denmark), 10*(8), pp. 982-993.

Sakamoto H, Rahman M, Nomura S, Okamoto E, Koike S, Yasunaga H et al. (2018) Japan Health System Review. Vol. 8 No. 1. New Delhi: World Health Organization, Regional Office for South-East Asia, 2018.

Sato, H., Hatanaka, K. C., Hatanaka, Y., Hatakeyama, H., Hashimoto, A., Matsuno, Y., Fukuda, S. and Sabe, H. (2014) High level expression of AMAP1 protein correlates with poor prognosis and survival after surgery of head and neck squamous cell carcinoma patients. *Cell Communication and Signaling, 12*(1), pp. 17.

Suzuki, T., Kondo, C., Kanamori, T. and Inouye, S. (2011) Video-Rate Bioluminescence Imaging of Matrix Metalloproteinase-2 Secreted from a Migrating Cell. *PLoS One, 6*(9), pp. e25243.

Tilokani, L., Nagashima, S., Paupe, V. and Prudent, J. (2018) Mitochondrial dynamics: overview of molecular mechanisms. *Essays Biochem, 62*(3), pp. 341-360.

Vander Heiden, M. G., Cantley, L. C. and Thompson, C. B. (2009) Understanding the Warburg effect: the metabolic requirements of cell proliferation. *Science, 324*(5930), pp. 1029-33.

Wai, T. and Langer, T. (2016) Mitochondrial Dynamics and Metabolic Regulation. *Trends in Endocrinology & Metabolism, 27*(2), pp. 105-117.

Wang, G., Mao, W. and Zheng, S. (2008) MicroRNA-183 regulates Ezrin expression in lung cancer cells. *FEBS Lett, 582*(25-26), pp. 3663-8.

Wang, S.-P., Wang, W.-L., Chang, Y.-L., Wu, C.-T., Chao, Y.-C., Kao, S.-H., Yuan, A., Lin, C.-W., Yang, S.-C., Chan, W.-K., et al. (2009) p53 controls cancer cell invasion by inducing the MDM2-mediated degradation of Slug. *Nature cell biology, 11*, pp. 694.

Westermann, B. (2010) Mitochondrial fusion and fission in cell life and death. *Nature Reviews Molecular Cell Biology, 11*, pp. 872.

Wolf, K., Mazo, I., Leung, H., Engelke, K., von Andrian, U. H., Deryugina, E. I., Strongin, A. Y., Brocker, E. B. and Friedl, P. (2003) Compensation mechanism in tumor cell migration: mesenchymal-amoeboid transition after blocking of pericellular proteolysis. *J Cell Biol, 160*(2), pp. 267-77.

Youle, R. J. and Narendra, D. P. (2010) Mechanisms of mitophagy. *Nature Reviews Molecular Cell Biology, 12*, pp. 9.

Yu, N., Fu, S., Liu, Y., Xu, Z., Liu, Y., Hao, J., Wang, B. and Zhang, A. (2015) miR-96 suppresses renal cell carcinoma invasion via downregulation of Ezrin expression. *Journal of Experimental & Clinical Cancer Research, 34*(1), pp. 107.

Yusa, K., Zhou, L., Li, M. A., Bradley, A. and Craig, N. L. (2011) A hyperactive piggyBac transposase for mammalian applications. *Proc Natl Acad Sci U S A, 108*(4), pp. 1531-6.

Zheng, X., Carstens, J. L., Kim, J., Scheible, M., Kaye, J., Sugimoto, H., Wu, C. C., LeBleu, V. S. and Kalluri, R. (2015) Epithelial-to-mesenchymal transition is dispensable for metastasis but induces chemoresistance in pancreatic cancer. *Nature, 527*(7579), pp. 525-530.

Zhu, J., Feng, Y., Ke, Z., Yang, Z., Zhou, J., Huang, X. and Wang, L. (2012) Down-Regulation of miR-183 Promotes Migration and Invasion of Osteosarcoma by Targeting Ezrin. *The American Journal of Pathology, 180*(6), pp. 2440-2451.